

ALMA MATER STUDIORUM · UNIVERSITY OF BOLOGNA

---

School of Science  
Department of Physics and Astronomy  
Master Degree in Physics

# On the Quantum Nature of Primordial Black Holes in Inflationary Cosmology

Supervisor:  
Dr. Roberto Casadio

Submitted by:  
Sayeda Tashnuba Jahan

Academic Year 2022/2023

## Abstract

In this thesis, we provide a quantum description to the formation of primordial black holes tackling the conventional methods of describing CMB anisotropies and formation of black holes in a semi-classical way. These primordial black holes arrive in nature at a very early stage of the universe soon after the end of inflation. We adopt a quantum field perspective to make an assumption of the size of these primordial black holes. Furthermore, we define the vacuum fluctuations of the Bunch-Davies type that arise during the inflationary epoch as a scalar perturbation field in curved space. Using the particle occupation of the vacuum state, we correlate the findings with a corpuscular theory of gravity to quantify our claim. This thesis works as a toy model to quantize primordial black holes from scalar perturbations left from inflation, therefore, this work can be adopted by various inflationary scenarios and similar early universe mechanisms that give rise to the same scale-invariant metric perturbations.

**Keywords:** Inflation, Cosmological Perturbation Theory, Quantum Field Theory in Curved Space-Time, Primordial Black Holes

## Acknowledgment

I am utterly grateful to my supervisor Prof. Roberto Casadio for the intellectual support, discussions and insights throughout this thesis. He has also helped me with building foundations required for this thesis through his course in Quantum Cosmology which has aggravated my knowledge in this work.

Furthermore, I would also like to acknowledge Prof. Michele Cicoli, Prof. Roberto Balbinot and Prof. Fiorenzo Bastianelli among many of my professors this year, who have taught me diligently and gave me an overall understanding of high-energy physics. It is due to all of them that my time in the University of Bologna was such an enlightening experience.

Additionally, I would like to express my deepest gratitude to my husband Ahmed Rakin Kamal for the various discussion sessions and emotional support throughout this time. My friends, Mishaal Hai, Noshin Ferdous Shamma, Tahsin Nahian Bin Quddus, Chiara Beccoï and Pujan Joshi have helped with their amazing existence, therefore, I would like to acknowledge them too.

Finally, this goes to my utmost support system, my father and my mother, who have instilled in me the courage to come here and pursue my passion, I would like to thank them with my achievements.

# Contents

<b>1</b>	<b>Introduction</b>	<b>4</b>
1.1	Outline . . . . .	4
1.2	Guide to the Thesis . . . . .	5
<b>2</b>	<b>Early Universe Cosmology</b>	<b>7</b>
2.1	The Homogeneous and Isotropic universe . . . . .	7
2.1.1	The Hubble Parameter and Redshift . . . . .	7
2.1.2	The Friedmann-Lemaitre-Robertson-Walker Metric . . . . .	8
2.1.3	The Einstein Equations . . . . .	9
2.1.4	Dynamics of an Expanding universe . . . . .	10
2.1.5	Equation of State . . . . .	11
2.1.6	The Horizon Scale . . . . .	13
2.2	The Composition of the Universe . . . . .	14
2.3	Problems of Hot Big Bang Cosmology . . . . .	18
2.3.1	The Horizon Problem . . . . .	18
2.3.2	The Flatness Problem . . . . .	19
2.3.3	Solution . . . . .	20
<b>3</b>	<b>Inflation and Cosmological Perturbations</b>	<b>21</b>
3.1	Single-Field Inflation . . . . .	21
3.1.1	The Slow-Roll Regime . . . . .	22
3.2	Cosmological Perturbations in the Inflationary Epoch . . . . .	23
3.2.1	The Scalar-Vector-Tensor Decomposition . . . . .	23
3.2.2	The Gauge Issue . . . . .	24
3.2.3	Perturbed Einstein Equations in Gauge-Invariant Form . . . . .	26
3.2.4	Curvature Perturbation . . . . .	27
3.2.5	Equation of Motion for Scalar Perturbations . . . . .	30
<b>4</b>	<b>Black Holes in the Early Universe</b>	<b>33</b>
4.1	Misner's Chaotic Cosmology . . . . .	33
4.2	Gravitationally Collapsed Objects of Very Low Mass . . . . .	34

4.3	Theoretical Framework of Primordial Black Holes . . . . .	34
4.3.1	PBH Formation as a Causal Process . . . . .	36
4.4	Thorne's Hoop Conjecture . . . . .	38
4.4.1	Threshold for Collapse . . . . .	39
4.5	Mass and Collapse Function of PBH at Formation . . . . .	39
<b>5</b>	<b>Quantum Fields in Curved Space-Time</b>	<b>42</b>
5.1	The Background Field Method . . . . .	42
5.1.1	The Vacuum Ambiguity . . . . .	43
5.1.2	Particle Creation in a Gravitational Background . . . . .	44
5.2	Bogolubov Transformation of Squeezed States . . . . .	46
5.2.1	The Unruh-DeWitt Particle Detector . . . . .	48
5.3	Semi-classicality and Decoherence of Momentum Modes . . . . .	50
5.3.1	Long-wave Mode Behaviour . . . . .	50
<b>6</b>	<b>Corpuscular Theory of Gravity</b>	<b>52</b>
6.1	Black Hole's Quantum N-Portrait . . . . .	52
6.2	Corpuscular Black Holes . . . . .	53
6.3	Black Holes as Bose-Einstein Condensates . . . . .	55
<b>7</b>	<b>Quantum Nature of Primordial Black Holes</b>	<b>56</b>
7.1	Linear Scalar Perturbations . . . . .	57
7.1.1	Quantization of the Perturbation Field . . . . .	58
7.2	Bogolubov Coefficients and Particle Density . . . . .	59
7.2.1	Exiting the Horizon . . . . .	60
7.3	Mukhanov-Sasaki Equation: Solution for Inflationary Models . . . . .	61
7.3.1	Quasi-isotropic Mode and Decaying Mode . . . . .	62
7.4	Null Particle Production at Reheating . . . . .	64
7.5	The Corpuscular Perspective . . . . .	65
<b>8</b>	<b>Conclusion</b>	<b>67</b>

# Chapter 1

## Introduction

### 1.1 Outline

Due to their non-baryonic nature and interaction signatures, primordial black holes stand to be the most probable source of dark matter we observe today, hence, understanding the nature of their creation would be helpful for modern cosmology. This thesis attempts to derive an interpretation of deeming the formation of primordial black holes from a quantum perspective.

Our work surrounds the idea that during the inflationary epoch, cosmological perturbations that go through decoherence and re-enter the horizon at a later stage, collapse to form primordial black holes. These primordial black holes form due to the horizon structure during re-entry that relates to the wavelength of the entering perturbations. This collapse is due to, mainly, scalar perturbations that arise as quantum fluctuations of the metric field in the background coupled to the inflaton field related to the accelerated expansion during inflation.

Primarily, we want to check if the same quasi-classical computations done for the CMB anisotropies and astrophysical black hole formation will be justified in such an early era of the universe. Given the size of the universe at the very beginning of these primordial black hole (PBH) formations, it is an educated guess that they might be of such sizes that should be interpreted as quantum. As the perturbation fields exit the horizon during a later stage of inflation, they receive inadequate time to occupy their vacuum states. This idea leads to the assumption that the fluctuations do not decoher outside the Hubble horizon but collapse to form quantum primordial black holes.

We approach this problem in a two-fold way. We consider linear scalar perturbations of the background metric field with a fluctuation term of the inflaton field in the longi-

tudinal gauge. We quantize this perturbation field as a quantum field theory in curved space-time. As the ambiguity in the vacuum states of this field will lead to generic particle creation around a gravitational background, we understand that these vacuum states will occupy once outside the Hubble horizon. Moreover, the overdensities in this field will, hence, collapse gravitationally to form primordial black holes upon horizon re-entry. Depending on the occupation of the vacuum states, the primordial black holes that form will vary in size. Therefore, if the vacuum states get minimal occupation, the size of the primordial black holes will be small. Hence, we believe a quasi-classical framework will not provide a complete description of these black holes.

Additionally, we approach this issue using the corpuscular picture in order to find the constituents for these PBHs using  $N$ , the occupation number of the Bose-Einstein Condensate corresponding object, which in our case are the black holes. We take a Gaussian probability of the collapse function and derive a relationship with the power spectrum of the quantum field. The power spectrum provides a description of the energy constituents that is related to the mass. The mass is related to the occupation number through the form  $N \sim \frac{M^2}{M_P^2}$ .

We successfully find a relationship of the particle density in regards to the time of black hole formation. We see that, indeed, at early times the particle occupation of the perturbation fields are small enough to be considered to form quantum black holes. A significance relationship with the formation of these black holes and decoherence time is established in this thesis.

The results of this work is fundamental to understanding the nature of primordial black holes. Through a bottom-up approach, we can further these assumptions to correlate quasi-classical structures that evolve as the universe expands. As the quantization procedure is dependent on the scale-invariant metric perturbations left from inflation, this research methodology can be adopted to several early universe cosmological models that leave behind similar perturbations. We can look into what this methodology results in different inflationary models, and even beyond inflationary cosmologies such as string influenced early universe models that leave behind similar seeds of structure formation.

## 1.2 Guide to the Thesis

The first chapter shall discuss the fundamentals of early universe cosmology that drives the concepts of the cosmological principle. We shall move on to the next chapter where we will discuss the inflationary theory and its importance in explaining the flaws in the homogeneous and isotropic Friedmann-Lemaître-Robertson-Walker universe.

Additionally, in the third chapter, we shall depict the basic foundations of our understanding of the formation of primordial black holes. The following chapters will pose fundamental prerequisites that lay the infrastructure of the work that has been done in the thesis. Furthermore, in the last chapters we present our original calculations that plaster our claim. Finally, we verify our model through a corpuscular approach.



# Chapter 2

## Early Universe Cosmology

In this chapter, we introduce the essential components necessary for understanding the early universe, particularly when considering the formation of Primordial Black Holes (PBHs). To begin, we provide a concise overview of the foundational concepts and theoretical framework used to describe a universe that is both homogeneous (uniform throughout) and isotropic (the same in all directions).

Next, we offer a brief account of the thermal history and the composition of the universe during various cosmic epochs. This involves explaining how the universe evolved in terms of temperature and the types of particles and matter present at different times.

Finally, we summarize the limitations of the Hot Big Bang theory, which led to the development of inflation theory. Inflation is regarded as the "standard theory" for describing the very early moments of cosmic history. It also serves as the source of primordial cosmological perturbations, which laid the groundwork for the large-scale structures we observe today and the lingering relic cosmic microwave background radiation.

### 2.1 The Homogeneous and Isotropic universe

#### 2.1.1 The Hubble Parameter and Redshift

It is widely accepted in cosmology that the universe is in a state of expansion. The rate at which this expansion occurs is characterized by a universal scale factor denoted as  $a(t)$ , which essentially holds all the relevant details regarding the universe's expansion history. This scale factor depends on cosmic time, denoted as  $t$ , which represents the time as measured by an observer who is at rest relative to the cosmic flow.

From the perspective of such a local observer, the distances they measure can be ex-

pressed as follows:

$$R(t) = a(t)r \quad (2.1)$$

where  $R(t)$  is the physical distance and  $r$  is the comoving distance. Similarly, one can define a useful time variable, denoted as  $\eta$ , which is defined as:

$$d\eta \equiv \frac{dt}{a(t)} \quad (2.2)$$

known as the conformal time. Naturally, one can also define the rate of the expansion of the universe, known as the Hubble parameter  $H$ , as

$$H = \frac{1}{a} \frac{da}{dt} = \frac{\dot{a}}{a} \quad (2.3)$$

The Hubble parameter, denoted as  $H$ , represents an essential concept in cosmology. It possesses dimensions of inverse time and holds significant importance as it provides a rough estimate of the age of the universe at the time it is measured. In contrast, the Hubble radius,  $cH^{-1}$  (where  $c$  is the speed of light), plays a crucial role in determining the size of the observable universe at the moment it is measured. Essentially, it defines the scale of causal contact within our universe.

When it comes to observations, scientists often gauge the universe's expansion using the redshift variable, denoted as  $z$ . This variable quantifies the relative change in the wavelength of a photon, symbolized as  $\frac{\Delta\lambda}{\lambda}$ , as it travels from its source to an observer. This change in wavelength is a direct result of the universe's expansion and can be expressed as:

$$1 + z \equiv \frac{a(t_{obs})}{a(t_{em})} \quad (2.4)$$

where  $a(t_{obs})$  and  $a(t_{em})$  are the scale factors at the times of observation and emission of the photons respectively. By measuring the redshifts  $z$ , e.g. in terms of luminosity distance, one can then reconstruct the expansion rate of the universe,  $H$ .

### 2.1.2 The Friedmann-Lemaitre-Robertson-Walker Metric

The Standard Hot Big Bang paradigm, is founded upon a fundamental concept called the cosmological principle. This principle asserts that, on large scales (approximately 100 million parsecs or more), the universe appears to be both spatially homogeneous (uniform) and isotropic (the same in all directions). There is observational evidence supporting this principle, with one remarkable piece of evidence being the nearly uniform temperature of the Cosmic Microwave Background (CMB) radiation observed from various parts of the sky.

When adopting the cosmological principle, it naturally constrains the mathematical description of the universe's geometry, specifically the infinitesimal line element between any two points in the universe. This description should accurately represent a universe that is both homogeneous and isotropic. The general form of this metric, known as the Friedmann-Lemaître-Robertson-Walker (FLRW) metric, is expressed as:

$$ds^2 \equiv g_{\mu\nu} dx^\mu dx^\nu = -dt^2 + a^2(t) \left[ \frac{dr^2}{1 - Kr^2} + r^2 (d\theta^2 + \sin^2 \theta d\phi^2) \right] \quad (2.5)$$

In this equation,  $g_{\mu\nu}$  represents the metric tensor, which is a mathematical construct used to describe the geometry of spacetime. The scale factor, denoted as  $a(t)$ , has units of length and describes how the size of the universe changes over time. The coordinates  $r$ ,  $\theta$ , and  $\phi$  are comoving coordinates, which are dimensionless and used to specify points in space relative to the observer's frame.

The variable  $K$  represents the spatial curvature signature of the metric. When  $K = 0$ , it indicates a flat universe, while  $K = \pm 1$  corresponds to a closed (spherical) universe and an open (hyperbolic) universe, respectively.

Expressed in terms of conformal time, the metric takes a particularly useful form. This form simplifies subsequent calculations and is given as follows:

$$ds^2 = -a^2(\eta) \left[ d\eta^2 + \frac{dr^2}{1 - Kr^2} + r^2 (d\theta^2 + \sin^2 \theta d\phi^2) \right] \quad (2.6)$$

Here, this metric equation describes the spacetime structure in a way that is advantageous for further analysis, especially when dealing with cosmological calculations.

### 2.1.3 The Einstein Equations

Once we've determined the infinitesimal line element in an expanding, homogeneous, and isotropic universe, we can establish a connection between the universe's expansion, which is a manifestation of spacetime curvature, and the energy-mass content of the universe. This connection is established through Einstein's equations of General Relativity (GR), which can be derived from the variation of an action, denoted as  $\mathcal{S}$ , that describes the entire universe. This action can be divided into two parts:  $\mathcal{S}_{\text{grav}}$  representing the gravitational aspect of the universe and  $\mathcal{S}_{\text{matter}}$  describing the matter content within the universe. These two parts are expressed as follows:

$$\mathcal{S}_{\text{grav}} = \frac{1}{16\pi G} \int d^4x \sqrt{-g} (R - 2\Lambda) \quad (2.7)$$

$$\mathcal{S}_{\text{matter}} = \int d^4x \sqrt{-g} \mathcal{L}_{\text{matter}} \quad (2.8)$$

Here, various symbols are defined as follows:  $G$  is the Newton constant,  $\Lambda$  is a cosmological constant,  $\mathcal{L}_{\text{matter}}$  represents the Lagrangian describing the matter content of the universe,  $g$  is the determinant of the metric tensor  $g_{\mu\nu}$ ,  $R$  is the Ricci scalar, defined as a contraction of the Ricci tensor  $R_{\mu\nu}$ , i.e.,  $R \equiv g_{\mu\nu} R^{\mu\nu}$ . The Ricci tensor  $R_{\mu\nu}$  is defined as  $R_{\mu\nu} \equiv \partial_\rho \Gamma_{\mu\nu}^\rho - \partial_\nu \Gamma_{\mu\rho}^\rho + \Gamma_{\mu\nu}^\rho \Gamma_{\rho\lambda}^\lambda - \Gamma_{\mu\lambda}^\rho \Gamma_{\nu\rho}^\lambda$ , where the Christoffel symbols are given by  $\Gamma_{\mu\nu}^\rho = \frac{g^{\rho\lambda}}{2} (\partial_\nu g_{\lambda\mu} + \partial_\mu g_{\lambda\nu} - \partial_\lambda g_{\mu\nu})$ .

By varying these two parts of the action, we obtain the following equations:

$$\frac{16\pi G}{\sqrt{-g}} \frac{\delta \mathcal{S}_{\text{grav}}}{\delta g_{\mu\nu}} = R_{\mu\nu} - \frac{1}{2} R g_{\mu\nu} + \Lambda g_{\mu\nu} \quad (2.9)$$

$$-\frac{2}{\sqrt{-g}} \frac{\delta \mathcal{S}_{\text{matter}}}{\delta g_{\mu\nu}} = g_{\mu\nu} \mathcal{L}_{\text{matter}} - 2 \frac{\partial \mathcal{L}_{\text{matter}}}{\partial g^{\mu\nu}} \quad (2.10)$$

Now, if we demand that  $\frac{\delta \mathcal{S}}{\delta g_{\mu\nu}} = \frac{\delta \mathcal{S}_{\text{grav}}}{\delta g_{\mu\nu}} + \frac{\delta \mathcal{S}_{\text{matter}}}{\delta g_{\mu\nu}} = 0$ , we arrive at Einstein's equations, given by:

$$G_{\mu\nu} + \Lambda g_{\mu\nu} = 8\pi G T_{\mu\nu} \quad (2.11)$$

In this equation, the Einstein tensor  $G_{\mu\nu}$  is defined as  $G_{\mu\nu} \equiv R_{\mu\nu} - \frac{1}{2} R g_{\mu\nu}$ , and the stress-energy tensor for matter is defined as:

$$T_{\mu\nu} \equiv -\frac{2}{\sqrt{-g}} \frac{\partial \mathcal{S}_{\text{matter}}}{\partial g_{\mu\nu}} \quad (2.12)$$

These equations represent the foundation of Einstein's theory of General Relativity and relate the curvature of spacetime (described by the metric tensor  $g_{\mu\nu}$ ) to the distribution of matter and energy in the universe.

### 2.1.4 Dynamics of an Expanding universe

Taking into account the cosmological principle and treating the universe's background medium as a perfect fluid, we can express the energy-momentum tensor in a general form:

$$T^{\mu\nu} = -p g^{\mu\nu} + (p + \rho) u^\mu u^\nu \quad (2.13)$$

Here,  $p$  and  $\rho$  represent the pressure and energy densities of the fluid, respectively, and  $u^\mu$  is the four-velocity of an observer at rest with respect to the homogeneous and isotropic space. Specifically, in the reference frame of (2.5),  $u^\mu$  equals  $\delta^{\mu 0}$ , where  $\delta$  is the

Kröneckers delta.

Solving Einstein's equations for a universe that is both homogeneous and isotropic, described by the FLRW metric, and filled with a perfect fluid as defined in the stress-energy tensor, we derive the following equations governing the evolution of the scale factor  $a(t)$  in such a universe:

$$\begin{aligned} H^2 &= \left(\frac{\dot{a}}{a}\right)^2 = \frac{\rho}{3M_{\text{Pl}}^2} - \frac{k}{a^2} + \frac{\Lambda}{3} && \text{Friedmann Equation} \\ \frac{\ddot{a}}{a} &= -\frac{4\pi G}{3}(\rho + 3p) + \frac{\Lambda}{3}, && \text{Raychaudhuri Equation} \end{aligned} \quad (2.14)$$

In these equations,  $H$  represents the Hubble parameter,  $\rho$  is the energy density,  $p$  is the pressure,  $k$  describes the spatial curvature, and  $\Lambda$  stands for the cosmological constant. We will use the definition of the reduced Planck mass as  $M_{\text{Pl}}^2 \equiv \frac{1}{8\pi G}$ .

It's noteworthy that combining the Friedmann and Raychaudhuri equations allows us to derive the continuity equation:

$$\dot{\rho} + 3H(\rho + p) = 0 \quad \text{Continuity Equation} \quad (2.15)$$

This equation can also be derived from the covariant conservation of the energy-momentum tensor, i.e.,  $\nabla_\mu T^{\mu\nu} = 0$ , and can be interpreted as the first law of thermodynamics,  $dU_{\text{th}} + p dV = 0$ , which describes an adiabatic expansion. Here,  $U_{\text{th}}$  represents the thermal energy density, defined as  $U_{\text{th}} \equiv \rho V$ , and  $V$  is the volume defined as  $V \equiv a^3$ .

Furthermore, we can express the Friedmann equation more concisely by introducing the dimensionless variable  $\Omega = \frac{\rho}{\rho_c}$ , where  $\rho_c = \frac{3H^2}{8\pi G}$  represents the critical energy density for a spatially flat universe. Consequently, we can reformulate the Friedmann equations as:

$$\Omega - 1 = \frac{K}{a^2 H^2} \quad (2.16)$$

and one can see that for  $K = -1$  (hyperbolic geometry),  $\Omega < 1$  whereas for  $K = +1$  (spherical geometry),  $\Omega > 1$ . Regarding the case in which  $K = 0$  (Euclidean geometry),  $\Omega = 1$  and the universe is spatially flat.

## 2.1.5 Equation of State

In this section, we delve into understanding how the scale factor of the universe evolves with respect to different components of its energy content, which can dominate during various cosmic epochs. We approach this by considering the dominant component as a perfect fluid, and we describe the thermal state of the universe using an equation of state of the form:

$$p = w\rho \quad (2.17)$$

Here,  $w$  serves as the equation-of-state parameter, determining the nature of this fluid. The scenario where  $w$  remains constant, which is often the focus of study, provides a good description of the universe's thermal state during different cosmic eras.

Assuming this constant equation-of-state parameter  $w = p/\rho$  for the universe's dominant component, we can derive the dynamics of both the universe's expansion and its energy density from the continuity equation and the Friedmann equation:

$$\begin{aligned} \rho &= \rho_{\text{ini}} \left( \frac{a}{a_{\text{ini}}} \right)^{-3(1+w)} \\ a &= \begin{cases} a_{\text{ini}} \left[ 1 \pm \frac{3}{2} \sqrt{\frac{\rho_{\text{ini}}}{3} \frac{t-t_{\text{ini}}}{M_{\text{P}}}} \right]^{\frac{2}{3(1+w)}} & \text{for } w \neq -1 \\ a_{\text{ini}} \exp \left\{ \left( \pm \sqrt{\frac{\rho_{\text{ini}}}{3} \frac{t-t_{\text{ini}}}{M_{\text{P}}}} \right) \right\} & \text{for } w = -1 \end{cases} \end{aligned} \quad (2.18)$$

Here, the 'ini' subscript indicates an initial time, and the '+' sign corresponds to an expanding universe with  $H$  (the Hubble parameter) greater than 0, while the '-' sign corresponds to a contracting universe with  $H$  less than 0.

Now, let's relate specific values of  $w$  to various thermal states of the universe at different cosmic epochs. When  $w = 0$ , it characterizes a fluid of non-relativistic particles, representing the matter-dominated era, where the energy density scales as  $\rho_{\text{m}} \sim a^{-3}$ . On the other hand, for  $w = 1/3$ , it describes a fluid of relativistic particles, representing the radiation-dominated era, with energy density scaling as  $\rho_{\text{r}} \sim a^{-4}$ . Lastly,  $w = -1$  characterizes a thermal state with negative pressure, where vacuum energy dominates the universe's energy content. This corresponds to the era of  $\Lambda$  (Lambda) domination, where the energy density of the cosmological constant  $\Lambda$ , denoted as  $\rho_{\Lambda}$ , remains constant. Similarly, the spatial curvature contributes to an energy density denoted as  $\rho_{\text{K}} = -\frac{3K}{a^2} M_{\text{P}}^2$ , which can be treated as the energy density of a perfect fluid with  $w = -1/3$ .

Taking all of this into account, we can reformulate the Friedmann equation in the following manner:

$$H^2 = \frac{1}{3M_{\text{P}}^2} (\rho_{\text{matter}} + \rho_{\text{K}} + \rho_{\Lambda}) = \frac{\rho_{\text{t}}}{3M_{\text{P}}^2}, \quad (2.19)$$

where  $\rho_{\text{matter}}$  accounts for the sum of the energy densities of ordinary matter, dark matter, radiation and any other constituent of the universe and  $\rho_{\text{t}}$  is the total energy density in the universe.

### 2.1.6 The Horizon Scale

In cosmology, the concept of the horizon is of fundamental importance. There are two main types of horizons: the cosmological or Hubble horizon (Hubble radius) and the particle horizon.

The Hubble horizon, denoted as  $R_{\text{H}}$ , is defined as:

$$R_{\text{H}} \equiv H^{-1} \quad (2.20)$$

This horizon represents the distance at which the velocity of recession of galaxies is equal to the speed of light. Galaxies beyond a sphere with a radius equal to the Hubble radius are moving away from us at speeds greater than the speed of light. This might seem to violate the principle of special relativity, which posits that the speed of light is the maximum speed in the universe. However, this doesn't contradict special relativity because it's the very fabric of spacetime that's expanding at a rate exceeding the speed of light, not objects within spacetime. Essentially, it's the stretching of space itself.

On the other hand, the particle horizon is defined as the region within which causal contact has been established through interactions involving photons. More precisely, at a given time, the particle horizon represents the extent of our past light cone at  $t = 0$ . Using the FLRW metric with  $d\theta = d\phi = 0$ , we can calculate the infinitesimal distance traveled by photons as  $dr = dt/a(t)$ . Therefore, the particle horizon, denoted as  $R_{\text{P}}$ , is defined as:

$$R_{\text{P}} \equiv a(t) \int_0^t \frac{dt'}{a(t')} \quad (2.21)$$

Assuming a polynomial behavior of the scale factor  $a(t)$  (i.e.,  $a(t) \propto t^n$  with  $n < 1$ , which is true for most cosmic epochs), it can be shown that  $R_{\text{P}}$  is approximately equal to  $H^{-1}$ . This means that the Hubble horizon and the particle horizon are of the same order, and they are often used interchangeably as the horizon scale, denoted as  $H^{-1}$ . This horizon scale provides a good estimate of the region where causal contact has been established and is also the scale at which general relativistic effects become significant.

Another relevant quantity is the horizon mass, denoted as  $M_{\text{H}}$ , which represents the mass enclosed within the horizon:

$$M_{\text{H}} \equiv \frac{4\pi}{3} \rho_{\text{t}} R_{\text{H}}^3 \quad (2.22)$$

Combining the form of the horizon mass and the Friedmann equation, it can be deduced that:

$$R_H = 2GM_H \tag{2.23}$$

In essence, these expressions link the horizon scale and horizon mass, providing valuable insights into the dynamics and scale of the universe.

The equation linking the mass enclosed within the horizon to the horizon scale bears a striking resemblance to the definition of the apparent horizon in black holes within spherical symmetry. This similarity highlights the shared physical characteristics of the cosmological horizon and the apparent horizon of black holes. Both can be considered as trapped surfaces in the framework of general relativity, signifying regions from which light cannot escape due to strong gravitational effects.

To emphasize, it's crucial to differentiate between physical lengths inside and outside the horizon, as this distinction leads to critical behaviours. Therefore, a length scale denoted as  $\lambda$  is related to these considerations.

The relationship between the wave number  $k$  and its corresponding comoving scale  $\lambda$  is such that the comoving scale associated with  $\lambda$  is equal to  $\lambda$  times the scale factor  $a$ . In mathematical terms, this can be expressed as  $\lambda = 2\pi a/k$ .

With this understanding, the conditions we have mentioned can be expressed as follows:

1. When  $k/(aH) \ll 1$ , it indicates that the scale  $\lambda$  is much larger than what is outside the horizon. In other words, it implies that the characteristic scale  $\lambda$  corresponds to physical phenomena that occur outside the horizon.
2. Conversely, when  $k/(aH) \gg 1$ , it signifies that the scale  $\lambda$  is much smaller than what is outside the horizon. In this case, the characteristic scale  $\lambda$  pertains to physical phenomena that occur inside the horizon.

These conditions help us categorize the scale of events or phenomena relative to the horizon scale and are crucial for understanding various cosmological processes.

## 2.2 The Composition of the Universe

In simpler terms, let's now explore how the universe's energy composition changes over time. We can break down each component of the universe's energy into what's essentially a perfect fluid. Assuming that there isn't significant energy transfer between these



components, we can calculate the total energy density of the universe by adding up the energy densities of these different components,

$$\rho_t = \sum_i \rho_{\text{ini},i} \left( \frac{a}{a_{\text{ini}}} \right)^{-3(1+w_i)}. \quad (2.24)$$

Here,  $i$  represents the various components that dominate during different cosmic epochs. By specifying the energy density of each component at a particular time, we can determine how  $\rho_t$  changes over time. To make this more concise, we introduce dimensionless parameters called  $\Omega_i$ . These parameters quantify the contribution of each component to the universe's energy budget and are defined as:

$$\Omega_i \equiv \frac{\rho_i}{\rho_c} \quad (2.25)$$

where  $\rho_c$  is the critical energy density required for a flat universe. In a nutshell, following the equations mentioned earlier, we can simplify in the following way:

$$\Omega_{\text{tot}} = \sum_i \Omega_i = 1 \quad (2.26)$$

Now, let's consider the  $\Omega$  parameters for the various constituents of the universe based on the findings from the Planck satellite's study of the Cosmic Microwave Background (CMB) relic radiation. Using these parameters along with equations above, we can reconstruct how the universe's composition has evolved over time.

1. **Baryonic Matter:** - This component represents ordinary matter in the form of cold baryons, such as protons and neutrons. These particles are heavier than leptons like electrons and neutrinos. According to the Planck 2018 results, their contribution is approximately  $\Omega_b^{(0)} \approx 0.049$ .

2. **Radiation:** - In this category, we account for relativistic particles, specifically CMB photons and neutrinos. Their overall contribution is exceedingly small, around  $\Omega_r^{(0)} \approx 10^{-4}$ .

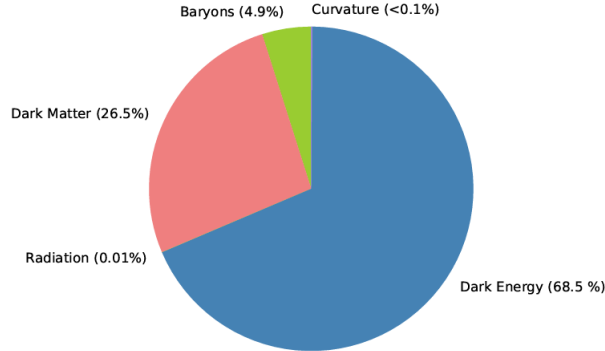


Figure 2.1: The composition of the universe today.[20]

3. **Dark Matter:** - Dark matter was postulated to explain various observations related to galaxy rotation curves and the formation of large-scale structures. This non-relativistic form of matter, described with  $w = 0$ , is non-baryonic in nature, and its exact properties remain a subject of ongoing research. Currently, it contributes  $\Omega_{\text{DM}}^{(0)} = 0.265$ , which is more than five times greater than the contribution of ordinary baryonic matter.

4. **Curvature:** - Using the Friedman equation and considering the definitions of the  $\Omega$  parameters, we can identify an  $\Omega$  parameter associated with spatial curvature. In cases where the universe is not flat (i.e., when  $K = \pm 1$ ), this curvature can be thought of as a fluid with  $w = -1/3$ . However, current observations are consistent with a spatially flat universe, with  $\Omega_K^{(0)} \approx 0$ . The current constraints on  $\Omega_K$  indicate that the universe is indeed very close to flat.

5. **Dark Energy:** - Dark energy is another fundamental component of the universe. It was hypothesized to exist, much like dark matter, to account for the missing large portion of the total energy density of the universe. Its existence gained prominence in the 1990s when observations indicated that the expansion of the universe was accelerating. This acceleration pointed to the presence of a mysterious energy component with a property referred to as the equation-of-state parameter, denoted as  $w$  being approximately equal to -1. This property is what led to the consideration of the cosmological constant, represented by  $\Lambda$ , as a leading candidate for dark energy.

Much like dark matter, the nature of dark energy remains a subject of active research in the field of cosmology. Currently, it is estimated that dark energy contributes significantly to the universe's total energy density, with a value of  $\Omega_{\text{DE}}^{(0)} \approx 0.685$  according to Planck 2018 findings.

Below we present the timeline of energy density domination of the universe in different epochs. Additionally, we also discuss the constituents of the universe in relation to the scale factor today,  $a_0$ .

By understanding the behavior of these non-interacting fluids representing different constituents of the universe, we can successfully reconstruct the thermal history of the cosmos, encompassing phases of radiation dominance, matter dominance, and the influence of dark energy. This is referred in Figure 2.2.

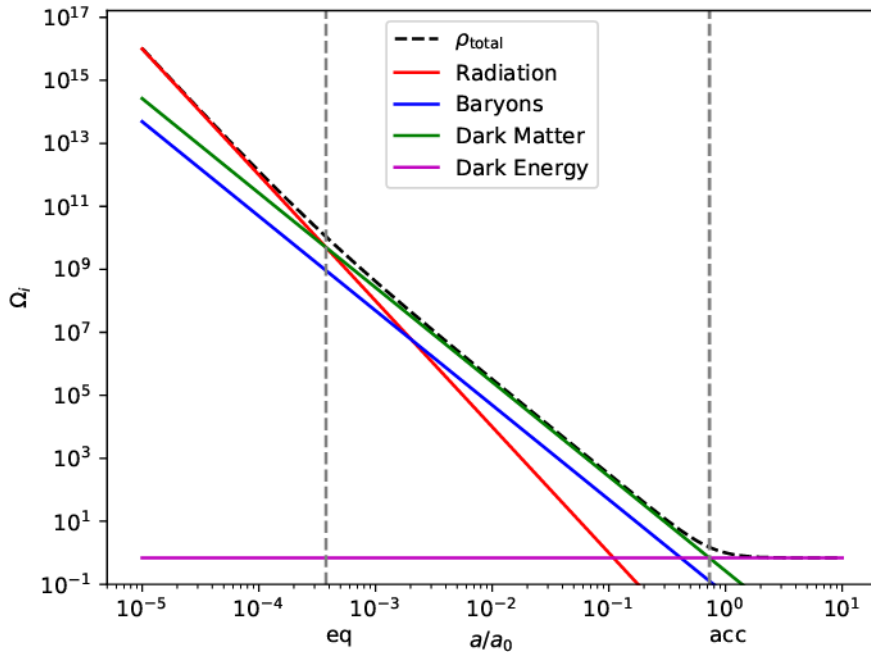


Figure 2.2: The dynamics of the energy density contribution of the different constituents of the universe.[20]

1. **Radiation Domination Era** ( $a < a_{eq}$ ): - In the early universe, there was a phase where radiation was the dominant energy component. During this phase, various phase transitions occurred, and thermal processes led to the formation of light elements and nuclei through primordial nucleosynthesis.
2. **Matter Domination Era** ( $a_{eq} < a < a_{acc}$ ): - Following the radiation-dominated phase, there was a transition to a period where matter, including dark matter, became the dominant component of the universe. During this time, large-scale

structures in the universe began to form due to the gravitational influence of matter.

3. **Dark Energy Era** ( $a > a_{\text{acc}}$ ): - In the later stages of the universe's evolution, dark energy started to play a significant role. This era is characterized by the accelerated expansion of the universe.

## 2.3 Problems of Hot Big Bang Cosmology

Here, we demonstrate the basic shortcomings of the Hot Big Bang Model that motivated inflation. We shall discuss primarily two of these problems; **The Horizon Problem** and **The Flatness Problem**.

### 2.3.1 The Horizon Problem

The horizon problem, also known as the large-scale homogeneity problem, can be summarized as follows: When we observe regions in the universe that are separated by distances greater than the speed of light multiplied by the age of the universe (meaning they are not causally connected), we find that these regions exhibit similar density and temperature fluctuations, even up to the order of  $10^{-5}$ . This observation appears to be contradictory because, according to the principles of special relativity, these regions should not have had the opportunity to influence each other due to the finite speed of light. Therefore, there seems to have been some form of information exchange between these distant regions in the past.

To delve into the quantitative aspects of this problem, we can examine how the horizon and physical lengths evolve during different cosmic epochs, particularly during the radiation domination (RD) and matter domination (MD) eras. For both of these eras, we can express the evolution of the Hubble horizon ( $R_H$ ) as follows:

During Radiation Domination (RD, where the equation of state parameter  $w = 1/3$ ):

$$R_H = \frac{4}{3} M_{\text{Pl}} \sqrt{\frac{3}{\rho_{\text{ini}}}} \left( 1 + \frac{3}{2} \sqrt{\frac{\rho_{\text{ini}}}{3}} \frac{t - t_{\text{ini}}}{M_{\text{Pl}}} \right) \quad (2.27)$$

During Matter Domination (MD, where  $w = 0$ ):

$$R_H = M_{\text{Pl}} \sqrt{\frac{3}{\rho_{\text{ini}}}} \left( 1 + \frac{3}{2} \sqrt{\frac{\rho_{\text{ini}}}{3}} \frac{t - t_{\text{ini}}}{M_{\text{Pl}}} \right) \quad (2.28)$$

In parallel, the evolution of physical distances ( $R_{\text{phys}}$ ) is expressed as:

For Radiation Domination (RD):

$$R_{\text{phys}} = a_{\text{ini}} \left( 1 + \frac{3}{2} \sqrt{\frac{\rho_{\text{ini}}}{3}} \frac{t - t_{\text{ini}}}{M_{\text{Pl}}} \right)^{1/2} \quad (2.29)$$

For Matter Domination (MD):

$$R_{\text{phys}} = a_{\text{ini}} \left( 1 + \frac{3}{2} \sqrt{\frac{\rho_{\text{ini}}}{3}} \frac{t - t_{\text{ini}}}{M_{\text{Pl}}} \right)^{2/3} \quad (2.30)$$

From these equations, it becomes evident that the Hubble horizon ( $R_H$ ) increases in size at a faster rate than physical distances during both the RD and MD eras. Consequently, in the early universe, there should have existed regions that were causally disconnected from each other due to the expansion. This disconnection should have resulted in variations in the observed properties of these regions, including density and temperature fluctuations. However, the actual observations show that our universe is remarkably homogeneous and isotropic, as evident from measurements such as the cosmic microwave background's temperature fluctuations ( $\frac{\delta T}{T} \sim 10^{-5}$ ) on angular scales larger than 1 degree, which corresponds to the horizon scale at the time the cosmic microwave background was emitted.

### 2.3.2 The Flatness Problem

In addressing the flatness problem, let's examine how the  $\Omega$  parameter, which is connected to the spatial curvature of the universe, evolves over time. We know that if the universe is perfectly flat today, then  $\Omega$  remains equal to 1 at all points in time. However, if there exists a small curvature, denoted as  $K$  and not equal to zero, then  $\Omega$  will vary with time. Let's focus on the scenario where  $K = +1$  (indicating positive spatial curvature) during the radiation domination (RD) and matter domination (MD) eras.

Understanding that the energy density of radiation  $\rho_r$  scales with the inverse fourth power of the scale factor ( $\propto a^{-4}$ ) during the RD era and that the energy density of matter  $\rho_m$  scales with the inverse cube of the scale factor ( $\propto a^{-3}$ ) during the MD era, we can utilize the relationship that  $H^2$  is proportional to the total energy density  $\rho_t$ . In this context, Equation (1.19) can be expressed as follows:

For Radiation Domination (RD):

$$\Omega - 1 \propto a^2 \quad (2.31)$$

For Matter Domination (MD):

$$\Omega - 1 \propto a \quad (2.32)$$

These expressions highlight how the deviation of  $\Omega$  from 1 (indicating the flatness of the universe) evolves over time. In the RD era, this deviation scales with  $a^2$ , while in the MD era, it scales linearly with  $a$ .

### 2.3.3 Solution

To tackle the horizon problem, the universe must have undergone a primordial phase where physical lengths, denoted as  $R_{\text{phys}}$ , expanded more rapidly than the horizon scale, marked by  $H^{-1}$ . Essentially, this condition ensures that photons, which might seem causally disconnected when considering the time of the Cosmic Microwave Background (CMB) emission, where  $\lambda > H^{-1}$  (with  $\lambda$  being the photon wavelength), had the opportunity to "communicate" during an early cosmic era where  $\lambda < H^{-1}$ . By meeting this requirement, we can explain the homogeneity and isotropy observed in the CMB, effectively addressing the horizon problem.

Mathematically, this condition can be expressed in terms of the scale factor's evolution, denoted as  $a(t)$ . Since  $\lambda \propto a$  and  $H^{-1} = a/\dot{a}$ , we need to ensure that during this early cosmic era, the following inequality holds:

$$\frac{d}{dt} \left( \frac{\lambda}{H^{-1}} \right) = \ddot{a} > 0. \quad (2.33)$$

This equation can be rewritten, using the Raychaudhuri equation and considering that this early cosmic era is dominated by a fluid  $X$  characterized by an equation-of-state parameter  $w_X = p/\rho$ , as follows:

$$w_X < -1/3. \quad (2.34)$$

To address the flatness/entropy problem, we must also require that in an initial cosmic era preceding the radiation era, the parameter  $\Omega - 1$  decreases, allowing for very low values, on the order of  $10^{-16}$ . To achieve this, we can assume that during this early era, the universe was dominated by a fluid  $X$  with the equation of state  $w_X$ . Combining the energy density equations from the section prior to this one, we can derive that:

$$\Omega - 1 \propto a^{1+3w_X}. \quad (2.35)$$

Consequently, to ensure that  $\Omega - 1$  decreases, we require:

$$w_X < -1/3. \quad (2.36)$$

Interestingly, this condition,  $w_X < -1/3$ , to address the flatness/entropy problem is the same condition that defines the inflationary period in cosmic expansion. During inflation, the universe undergoes accelerated expansion ( $\ddot{a} > 0$ ), and the  $\Omega$  parameter at the end of inflation is driven very close to, but not exactly at, one, regardless of its initial value.

# Chapter 3

## Inflation and Cosmological Perturbations

In this chapter, we revisit the fundamentals of the theory of inflation, which, as mentioned in Chapter 2, provides solutions to a variety of fundamental issues within the framework of the Hot Big Bang theory. We begin by summarizing the standard single-field slow-roll inflation paradigm. Subsequently, we provide a brief overview of the theory of cosmological inflationary perturbations, which are responsible for seeding the Primordial Black Holes (PBHs) studied within the context of this thesis.

### 3.1 Single-Field Inflation

This era characterized by negative pressure can naturally occur within the framework of single-field inflation, where a scalar field called the inflaton field, denoted as  $\phi$ , is minimally coupled to gravity. The action that describes this scalar field is given by:

$$\mathcal{S}_\phi = \int d^4x \sqrt{-g} \left[ \frac{1}{2} \partial_\mu \phi \partial^\mu \phi + V(\phi) \right], \quad (3.1)$$

In this action, the first term represents the kinetic energy of the scalar field, while the second term represents its potential energy. The stress-energy tensor associated with this action can be obtained by substituting  $\mathcal{S}_{\text{matter}}$  with  $\mathcal{S}_\phi$  and is defined as:

$$T_{\mu\nu}^{(\phi)} = \partial_\mu \phi \partial_\nu \phi + g_{\mu\nu} \left[ -\frac{1}{2} g^{\rho\sigma} \partial_\rho \phi \partial_\sigma \phi + V(\phi) \right]. \quad (3.2)$$

Since we are working within the framework of a FLRW background, the inflaton field  $\phi$  is expected to be homogeneous, meaning it only depends on time. Consequently, the energy and pressure densities of the inflaton field can be derived from  $T_{\mu\nu}^{(\phi)}$  and are given as follows:

$$\begin{aligned}\rho_\phi = T_{00} &= \frac{\dot{\phi}^2}{2} + V(\phi), \\ p_\phi = T_{ii} &= \frac{\dot{\phi}^2}{2} - V(\phi).\end{aligned}\tag{3.3}$$

In order for a homogeneous scalar field to drive a period of accelerated expansion, which characterizes inflation ( $3p + \rho < 0$ ), the potential  $V(\phi)$  must satisfy the condition:

$$V(\phi) > \dot{\phi}^2.\tag{3.4}$$

This condition ensures that for inflation to occur, the inflaton field must slowly roll down its potential so that its potential energy dominates over its kinetic energy.

Now, let's delve into the background dynamics of the inflaton field. We can derive this by substituting the energy density and pressure equations above into the continuity equation. This leads to the Klein-Gordon equation for  $\phi$ :

$$\ddot{\phi} + 3H\dot{\phi} + V_\phi(\phi) = 0,\tag{3.5}$$

where  $V_\phi(\phi)$  is defined as the derivative of the potential  $V(\phi)$  with respect to  $\phi$ .

Additionally, considering the Friedmann equation, it can be expressed as:

$$3M_{\text{Pl}}^2 H^2 = V(\phi) + \frac{\dot{\phi}^2}{2},\tag{3.6}$$

Here,  $M_{\text{Pl}}$  represents the reduced Planck mass. These equations describe the background dynamics of the inflaton field during inflation, highlighting the relationship between the field's kinetic and potential energy, as well as its evolution over time.

### 3.1.1 The Slow-Roll Regime

The slow-roll regime is defined when  $V(\phi) \gg \dot{\phi}^2$ . In such a case, one gets from the energy density and pressure equations that  $p_\phi \simeq -\rho_\phi$ . According to the continuity equation, the energy density  $\rho$  remains almost constant over time. Similarly, from the Friedmann equation, the Hubble parameter  $H$  also exhibits minimal variation over time. This leads the spacetime to resemble a de Sitter universe, which is essentially a universe dominated by a cosmological constant.

The slow-roll regime represents a situation where the universe is perturbatively close to a de Sitter universe. This particular limit is of great interest because it aligns with observational evidence indicating an almost scale-invariant power spectrum on the scales



of the Cosmic Microwave Background (CMB), consistent with predictions from the slow-roll single-field inflation model.

To quantify how closely the universe deviates from a de Sitter universe during the slow-roll regime, slow-roll parameters are introduced. These parameters allow for a perturbative expansion of the curvature power spectrum. Among various sets of slow-roll parameters, the Hubble-flow parameters, denoted as  $\epsilon_n$ , are widely used in the literature. They are iteratively defined as follows:

$$\epsilon_{n+1} = \frac{d \ln |\epsilon_n|}{dN}, \quad (3.7)$$

where  $N$  represents a time variable referred to as the e-fold number, defined as the natural logarithm of the scale factor,  $N \equiv \ln a$ . In this parameterization,  $\epsilon_0$  is defined as  $\epsilon_0 = H_{ini}/H$ , where "ini" signifies an initial time. In the case of a de Sitter universe,  $\epsilon_0$  is a constant with a value of 1. Therefore, in the slow-roll regime, which describes an almost de Sitter universe,  $\epsilon_0$  should remain nearly constant over time, close to 1, and its time derivatives, calculated through the equation above, should be small. This characteristic makes the slow-roll parameters invaluable for describing perturbations away from de Sitter expansion. In the language of slow-roll parameters, one can define slow-roll inflation as long as  $|\epsilon_n| \ll 1$  for all  $n > 0$ .

## 3.2 Cosmological Perturbations in the Inflationary Epoch

Inflation stands as the conventional theory for explaining the early stages of cosmic history. This is primarily because the primordial cosmological perturbations generated during inflation play a pivotal role in seeding the formation of the large-scale structures we observe in the universe today, as well as contributing to the anisotropies observed in the cosmic microwave background radiation, a relic from the early universe. Consequently, in this section, we will provide an overview of the theory of cosmological inflationary perturbations, which serves as a fundamental pillar of modern cosmology.

### 3.2.1 The Scalar-Vector-Tensor Decomposition

To introduce cosmological perturbations atop a homogeneous and isotropic background universe, we need to move beyond perfect homogeneity and isotropy. The most general perturbed metric capable of describing small deviations from a FLRW universe can be expressed as follows:

$$ds^2 = a^2(\eta) \left[ - (1 + 2A)d\eta^2 + 2B_i dx^i d\eta + (\gamma_{ij} + h_{ij}) dx^i dx^j \right], \quad (3.8)$$

Here,  $A$ ,  $B_i$ , and  $h_{ij}$  are functions of both space and time, representing the deviations from a perfectly homogeneous and isotropic universe.  $\gamma_{ij}$  represents the spatial part of the background metric. In the case of a flat FLRW background universe, as we are considering,  $\gamma_{ij} = \delta_{ij}$ .

To understand the dynamics of these cosmological perturbations, it's convenient to decompose them into scalar, vector, and tensor components, which is why this decomposition is often referred to as Scalar-Vector-Tensor (SVT) decomposition. Specifically, any vector field  $B_i$  can be decomposed into the divergence of a scalar field  $B$  and a vector field  $\bar{B}_i$  with zero divergence:

$$B_i = \partial_i B + \bar{B}_i, \quad \text{where } \partial^i \bar{B}_i = 0. \quad (3.9)$$

Similarly, any tensor field  $h_{ij}$  can be decomposed into components as follows:

$$h_{ij} = -2\psi\gamma_{ij} + 2\partial_i\partial_j E + 2\partial_{(i}\bar{E}_{j)} + 2\bar{E}_{ij}, \quad (3.10)$$

Here,  $\partial_i \bar{E}^{ij} = 0$  and  $\bar{E}_i^i = 0$ .

Vector perturbations tend to be rapidly suppressed during the inflationary stage, so they are often neglected. In contrast, scalar and tensor perturbations receive significant attention. Concentrating on scalar perturbations at the linear order and using the SVT decomposition described earlier, the metric with small perturbations can be expressed as follows:

$$ds^2 = a^2(\eta) \left[ - (1 + 2A)d\eta^2 + 2\partial_i B dx^i d\eta + [(1 - 2\psi)\delta_{ij} + 2\partial_i\partial_j E] dx^i dx^j \right], \quad (3.11)$$

Here, we have substituted  $\gamma_{ij} = \delta_{ij}$ , considering the observed negligible spatial curvature, which favors a flat FLRW background universe.

### 3.2.2 The Gauge Issue

The study of cosmological perturbations involves comparing physical quantities between two different spacetimes: one that adheres to the cosmological principle of being homogeneous and isotropic (the FLRW metric) and another where this principle does not

strictly apply. To compute perturbations in a physical quantity, we need to compare its values in both the unperturbed background spacetime and the perturbed spacetime at the same spacetime point. Since these values exist in different spacetime geometries, we must establish a correspondence between them, known as a gauge choice. Fixing a gauge is akin to selecting a specific threading into lines (representing fixed spatial coordinates) and a slicing into hypersurfaces (representing fixed time).

Consider an infinitesimal coordinate or gauge transformation represented by:

$$x^\mu \rightarrow \tilde{x}^\mu = x^\mu + \xi^\mu, \quad (3.12)$$

where  $\xi^\mu = (\xi^0, \xi^i)$  is a four-vector with components  $\xi^0$  and  $\xi^i$  that depend on both space and time. As discussed previously, any vector field  $\xi^i$  can be decomposed into the divergence of a scalar field,  $\xi$ , and a vector field,  $\xi_{\text{tr}}^i$ , with a vanishing divergence ( $\xi_{\text{tr},i}^i = 0$ ). This decomposition allows us to write the transformation as:

$$\tilde{x}^0 = x^0 + \xi^0(x^0, x^i), \quad \tilde{x}^i = x^i + \gamma^{ij} \xi_{;j}(x^0, x^i), \quad (3.13)$$

where the comma denotes the covariant derivative with respect to the background space coordinates. Focusing on functions  $\xi^0$  and  $\xi$  that preserve the scalar nature of metric perturbations, we can express this transformation as follows:

$$\begin{aligned} \tilde{A} &= A - \frac{a'}{a} \xi^0 - \xi^{0'}, \\ \tilde{\psi} &= \psi + \frac{a'}{a} \xi^0, \\ \tilde{B} &= B + \xi^0 - \xi', \\ \tilde{E} &= E - \xi, \end{aligned} \quad (3.14)$$

where the prime denotes a derivative with respect to conformal time  $\eta$ .

The challenge that arises with gauge choice is that there isn't a single preferred gauge. This means there is no unique choice for the functions  $A, B, \psi$ , and  $E$ . To address this, two general approaches are typically employed:

1. Use gauge-invariant quantities for all calculations.
2. Make a specific gauge choice and perform calculations within that gauge.

Both approaches have their advantages and disadvantages. Opting for a specific gauge can simplify computations but may introduce gauge artifacts. Conversely, working with gauge-invariant quantities avoids gauge-related issues but might lead to more complex calculations in some cases. The choice depends on the specific problem and the trade-offs

involved.

On the other hand, opting for gauge-invariant computations, although potentially more complex, offers the benefit of working exclusively with physical quantities. Gauge-invariant quantities can be constructed by combining the perturbation variables  $A, B, \psi$ , and  $E$  in various ways.

Among the simplest and most important gauge-invariant quantities in the gravitational sector are the Bardeen potentials, denoted as  $\Phi$  and  $\Psi$ , and defined as follows:

- $\Phi$  is a combination of  $A, B, E$ , and their derivatives, designed to capture gravitational perturbations.
- $\Psi$  similarly accounts for gravitational perturbations but also depends on the scale factor and its derivative.

In situations where there is no anisotropic stress, meaning no off-diagonal space-space components in the stress-energy tensor, it can be shown that  $\Phi$  is equal to  $\Psi$ .

For the matter sector, particularly in the context of scalar fields like  $\phi$ , gauge-invariant fluctuations can be constructed as well. These gauge-invariant scalar fluctuations are denoted as  $\delta\phi^{(\text{gi})}$  and are formed by combining  $\delta\phi$  (the perturbation in the scalar field) with derivatives of  $\phi$  and the perturbation variables  $B$  and  $E$ .

Moreover, gauge-invariant scalar fluctuations for other scalar quantities, such as energy density ( $\rho$ ) and pressure ( $p$ ), can also be defined using a similar approach. Specifically, given a scalar quantity  $f$ , you can create a gauge-invariant fluctuation  $\delta f^{(\text{gi})}$  by combining  $\delta f$  with derivatives of  $f, B$ , and  $E$ .

It's worth noting that while the construction of  $\delta f^{(\text{gi})}$  is commonly used in the literature, there are numerous other possible ways to define gauge-invariant scalar fluctuations.

### 3.2.3 Perturbed Einstein Equations in Gauge-Invariant Form

The connection between matter and metric fluctuations emerges from Einstein's equations. Utilizing gauge-invariant quantities and under the assumption of no anisotropic stress ( $\Phi = \Psi$ ), the perturbed Einstein's equations ( $\delta G_{\mu\nu}^{(\text{gi})} = 8\pi\delta T_{\mu\nu}^{(\text{gi})}$ ) can be derived after some involved calculations as follows:

For the temporal-temporal component:

$$\nabla^2\Phi - 3\mathcal{H}\Phi' - 3\mathcal{H}^2\Phi = \frac{a^2}{2M_{\text{Pl}}^2}\delta T_0^{(\text{gi})0} \quad (3.15)$$

For the spatial-temporal component:

$$\partial_i(\Phi' + \mathcal{H}\Phi) = \frac{a^2}{2M_{\text{Pl}}^2}\delta T_i^{(\text{gi})0} \quad (3.16)$$

For the spatial-spatial component:

$$[\Phi'' + 3\mathcal{H}\Phi' + (2\mathcal{H}' + \mathcal{H}^2)\Phi]\delta_j^i = -\frac{a^2}{2M_{\text{Pl}}^2}\delta T_j^{(\text{gi})i} \quad (3.17)$$

Considering the perturbed stress-energy tensor of the inflaton field, the components can be written as expressions involving gauge-invariant perturbations  $\delta\phi^{(\text{gi})}$  and  $\Phi$ . Substituting these into the equations above yields:

For the temporal-temporal component:

$$\nabla^2\Phi - 3\mathcal{H}\Phi' - 3\mathcal{H}^2\Phi = \frac{1}{2M_{\text{Pl}}^2}(-\phi'^2\Phi + \phi'\delta\phi^{(\text{gi})'} + V_{,\phi}(\phi)a^2\delta\phi^{(\text{gi})}) \quad (3.18)$$

For the spatial-temporal component:

$$(\Phi' + \mathcal{H}\Phi) = \frac{1}{2M_{\text{Pl}}^2}\phi'\delta\phi^{(\text{gi})} \quad (3.19)$$

For the spatial-spatial component:

$$\Phi'' + 3\mathcal{H}\Phi' + (2\mathcal{H}' + \mathcal{H}^2)\Phi = -\frac{1}{2M_{\text{Pl}}^2}(\phi'^2\Phi - \phi'\delta\phi^{(\text{gi})'} + V_{,\phi}(\phi)a^2\delta\phi^{(\text{gi})}) \quad (3.20)$$

Using these equations and incorporating the Klein-Gordon equation, an equation describing the dynamics of  $\Phi$  in the gravitational sector can be obtained:

$$\Phi'' + 2\left(\mathcal{H} - \frac{\phi''}{\phi'}\right)\Phi' - \nabla^2\Phi + 2\left(\mathcal{H}' - \mathcal{H}\frac{\phi''}{\phi'}\right)\Phi = 0 \quad (3.21)$$

### 3.2.4 Curvature Perturbation

In the preceding discussion, we observed that matter perturbations, specifically the perturbations in the scalar field denoted as  $\delta\phi^{(\text{gi})}$ , act as sources for metric perturbations represented by  $\Phi$  through the Einstein equations. These metric perturbations, when

translated, result in perturbations in the curvature of spacetime. These spacetime curvature perturbations are profoundly significant because they are instrumental in explaining key phenomena such as the large-scale structure and the anisotropies observed in the cosmic microwave background (CMB) radiation.

In this section, we will introduce the concept of curvature perturbations in two widely studied gauges and then proceed to construct gauge-invariant curvature perturbations based on these two gauges.

### The Comoving Curvature Perturbation:

The function  $\psi$ , which appears in the spatial part of perturbed metrics, is associated with the intrinsic curvature of hypersurfaces at constant time. Specifically, when dealing with a flat FLRW background, we can establish a relationship between the spatial Ricci scalar, denoted as  ${}^{(3)}R$  and defined as  ${}^{(3)}R \equiv \gamma^{ij} R_{ij}$ , and the perturbation  $\psi$  as follows:

$${}^{(3)}R = \frac{4}{a^2} \nabla^2 \psi \quad (3.22)$$

The comoving curvature perturbation, denoted as  $\mathcal{R}$ , is defined as the metric perturbation  $\psi$  in the comoving slicing gauge. This gauge corresponds to the perspective of freely falling comoving observers in which the expansion of the universe is isotropic. Importantly, in this gauge, comoving observers do not measure any energy flux, which is represented as  $T_i^0 = 0$ . Consequently,  $\mathcal{R}$  is formally defined as:

$$\mathcal{R} \equiv \psi|_{T_i^0=0} \quad (3.23)$$

The expression for  $\mathcal{R}$  can be generalized to any gauge by considering a gauge transformation on constant time surfaces, where  $\eta$  is shifted by  $\delta\eta$ . Under this transformation, the perturbation  $\psi$  changes, with  $\xi^0 = \delta\eta$ , resulting in the following transformation:

$$\psi \rightarrow \tilde{\psi} = \psi + \mathcal{H}\delta\eta.$$

In the comoving gauge, where  $T_i^0 = 0$ , and noting that at the background level  ${}^{(0)}T_i^0 = 0$ , and that  $\delta T_i^{(gi)0} \propto \partial_i \delta\phi\phi'$ , we find that the fluctuation for the scalar field  $\phi$  in the comoving gauge,  $\delta\phi_{\text{com}}$ , becomes zero:  $\delta\phi_{\text{com}} = 0$ .

To proceed further and derive the expression for  $\mathcal{R}$  in a general gauge, we need to understand how a scalar fluctuation, such as  $\delta\phi$ , transforms under a gauge transformation.

Let  $f$  be a scalar quantity, and consider the generic coordinate transformation given above. Since  $f$  is scalar, its value at a physical point remains consistent across all coordinate systems. Therefore,  $\tilde{f}(\tilde{x}^\mu) = f(x^\mu)$ . Additionally, for the unperturbed background,

$f_0(x^\mu) = \tilde{f}_0(x^\mu)$ , where the subscript 0 denotes background quantities. Consequently, we can deduce how the scalar fluctuation  $\delta f(x^\mu) \equiv f(x^\mu) - f_0(x^\mu)$  transforms under a general coordinate transformation. Specifically:

$$\begin{aligned}
\tilde{\delta f}(\tilde{x}^\mu) &= \tilde{f}(\tilde{x}^\mu) - \tilde{f}_0(\tilde{x}^\mu) \\
&= f(x^\mu) - f_0(\tilde{x}^\mu) \\
&= f(\tilde{x}^\mu) - \delta x^\mu \frac{\partial f}{\partial x^\mu}(\tilde{x}^\mu) - f_0(\tilde{x}^\mu) \\
&\simeq \delta f(\tilde{x}^\mu) - \delta x^\mu \frac{\partial}{\partial x^\mu} (f_0(\tilde{x}^\mu) + \delta f(\tilde{x}^\mu)),
\end{aligned} \tag{3.24}$$

where the last equality involves a first-order expansion of the function  $f(\tilde{x}^\mu)$ . Given that, for a homogeneous and isotropic scalar field, the background function  $f_0$  depends only on time, and considering first-order contributions,  $\tilde{\delta f}(\tilde{x}^\mu)$  can be expressed as:

$$\tilde{\delta f}(\tilde{x}^\mu) = \delta f(x^\mu) - f'_0 \delta \eta. \tag{3.25}$$

Hence, based on the aforementioned derivation, the transformation of  $\delta \phi$  can be expressed as  $\delta \phi \rightarrow \delta \phi - \phi' \delta \eta$ . Consequently, for a transformation occurring on constant time hypersurfaces, we obtain:

$$\delta \phi \rightarrow \delta \phi_{\text{com}} = \delta \phi - \phi' \delta \eta = 0 \Leftrightarrow \delta \eta = \frac{\delta \phi}{\phi'}. \tag{3.26}$$

As a result, the comoving curvature perturbation, denoted as  $\mathcal{R}$ , can be defined in any gauge as:

$$\mathcal{R} \equiv \psi + \mathcal{H} \frac{\delta \phi}{\phi'}. \tag{3.27}$$

where  $\mathcal{H}$  is the comoving Hubble parameter defined by

$$\mathcal{H} = \frac{a'}{a}$$

where the derivative on the scale factor is with respect to conformal time.

It's crucial to emphasize that the quantity defined above is inherently gauge-invariant. Therefore,  $\mathcal{R}$  serves as the gravitational potential on hypersurfaces where  $\delta \phi = 0$ , which can be expressed as:

$$\mathcal{R} = \psi|_{\delta \phi=0}. \tag{3.28}$$

Additionally, it's worth highlighting the practicality of the comoving curvature perturbation, particularly its constancy on large scales. This constancy enables it to be used for propagating the inflationary power spectrum from the end of inflation to the post-inflationary era.

### The uniform energy density curvature perturbation :

Similarly, we can introduce the uniform energy density curvature perturbation, denoted as  $\zeta$ , by adopting a slicing where  $\delta\rho = 0$ . Thus,  $\zeta$  is formally defined as:

$$\zeta \equiv \psi|_{\delta\rho=0}. \quad (3.29)$$

When we perform a transformation on hypersurfaces of constant time, considering that  $\delta\rho$  is a scalar fluctuation, it transforms as  $\delta\rho \rightarrow \delta\rho - \rho'\delta\eta$ . Following a similar line of reasoning as in the case of the comoving slicing, we find that in the uniform energy density slicing,  $\delta\eta$  can be expressed as  $\delta\eta = \frac{\delta\rho}{\rho'}$ . Consequently, in any arbitrary gauge, we can define  $\zeta$  as:

$$\zeta \equiv \psi + \mathcal{H} \frac{\delta\rho}{\rho'}, \quad (3.30)$$

and it retains its gauge-invariant nature by design. It's worth noting that, on superhorizon scales (where  $k \ll aH$ ), the curvature perturbation in the uniform energy density gauge,  $\zeta$ , is equivalent to the comoving curvature perturbation,  $\mathcal{R}$ .

### 3.2.5 Equation of Motion for Scalar Perturbations

In the preceding section, we introduced two key quantities: the Bardeen potentials, denoted as  $\Phi$  and  $\Psi$ , and the gauge-invariant inflaton perturbation,  $\delta\phi^{(\text{gi})}$ . These gauge-invariant variables describe the gravitational and matter sectors, respectively, and are interconnected through the Einstein equations. This implies the possibility of constructing a gauge-invariant quantity that uniquely represents both the scalar sectors, i.e., both gravitational and matter components. To this end, we introduce the Mukhanov-Sasaki variable, denoted as  $v(\eta, \mathbf{x})$ , which is a combination of the Bardeen potential and the gauge-invariant inflaton perturbation  $\delta\phi^{(\text{gi})}$ , defined as follows:

$$v(\eta, \mathbf{x}) = a \left( \delta\phi^{(\text{gi})} + \phi' \frac{\Phi}{\mathcal{H}} \right). \quad (3.31)$$

It's noteworthy that the Mukhanov-Sasaki variable is connected to the comoving curvature perturbation  $\mathcal{R}$  through the relationship:

$$v = \frac{a\phi'}{\mathcal{H}} \mathcal{R}. \quad (3.32)$$

This equation is gauge-invariant and is established by starting in the Newtonian gauge (where  $E = B = 0$  and  $\Psi = \psi$ ) and considering that  $\Phi = \Psi$  when there's no anisotropic stress.

To derive the equation of motion for  $u(\eta, \mathbf{x})$ , we need to construct the total action



for the system, which is the sum of the gravitational sector's action (the Einstein-Hilbert action) and the action for the matter sector (inflaton scalar field action). By expanding this action up to second order in perturbations, a somewhat lengthy calculation yields:

$${}^{(2)}\delta\mathcal{S} = \frac{1}{2} \int d^4x \left[ v'^2 - \delta^{ij} \partial_i v \partial_j v + \frac{(a\sqrt{\epsilon_1})''}{a\sqrt{\epsilon_1}} u^2 \right], \quad (3.33)$$

where  $\epsilon_1$  is the first slow-roll parameter.

Next, to express the action in terms of the Fourier modes of  $v(\eta, \mathbf{x})$ , we consider that, in the context of linear theory, each mode evolves independently. Therefore, by expanding  $v(\eta, \mathbf{x})$  into Fourier modes, we obtain:

$$v(\eta, \mathbf{x}) = \frac{1}{(2\pi)^{3/2}} \int_{\mathbb{R}} d^3\mathbf{k} v_{\mathbf{k}}(\eta) e^{i\mathbf{k}\cdot\mathbf{x}}, \quad (3.34)$$

where  $v_{-\mathbf{k}} = v_{\mathbf{k}}^*$  because  $v(\eta, \mathbf{x})$  is real. Substituting this, we find:

$${}^{(2)}\delta\mathcal{S} = \int d\eta \int_{\mathbb{R}^+ \times \mathbb{R}^2} d^3\mathbf{k} \left\{ v'_{\mathbf{k}} v_{\mathbf{k}}^* + v_{\mathbf{k}} v_{\mathbf{k}}^* \left[ \frac{(a\sqrt{\epsilon_1})''}{a\sqrt{\epsilon_1}} - k^2 \right] \right\}, \quad (3.35)$$

where the integral is taken over the positive half of the Fourier space due to the redundancy  $v_{-\mathbf{k}} = v_{\mathbf{k}}^*$ . Therefore, the Lagrangian density in Fourier space can be expressed as:

$$\mathcal{L} \equiv \int_{\mathbb{R}^+ \times \mathbb{R}^2} d^3\mathbf{k} \left\{ v'_{\mathbf{k}} v_{\mathbf{k}}^* + v_{\mathbf{k}} v_{\mathbf{k}}^* \left[ \frac{(a\sqrt{\epsilon_1})''}{a\sqrt{\epsilon_1}} - k^2 \right] \right\}. \quad (3.36)$$

With the conjugate momentum  $p_{\mathbf{k}}$  defined as:

$$p_{\mathbf{k}} \equiv \frac{\delta\mathcal{L}}{\delta v_{\mathbf{k}}^*} = v'_{\mathbf{k}}, \quad (3.37)$$

the Laplace equation, derived from minimizing the action  ${}^{(2)}\delta\mathcal{S}$ , can be expressed as:

$$\frac{\partial\mathcal{L}}{\partial v_{\mathbf{k}}^*} = \frac{\partial\mathcal{L}}{\partial p_{\mathbf{k}}^*}, \quad (3.38)$$

which leads to the equation of motion for the Mukhanov-Sasaki variable:

$$v_{\mathbf{k}}'' + \left( k^2 - \frac{(a\sqrt{\epsilon_1})''}{a\sqrt{\epsilon_1}} \right) v_{\mathbf{k}} = 0. \quad (3.39)$$

From the equation above, it's evident that each mode  $\mathbf{k}$  behaves like a parametric oscillator with a time-varying frequency  $\omega(\eta, \mathbf{k})$ , given by:

$$\omega^2(\eta, k) = k^2 - \frac{(a\sqrt{\epsilon_1})''}{a\sqrt{\epsilon_1}}. \quad (3.40)$$

It's apparent that the frequency  $\omega(\eta, \mathbf{k})$  is dependent on the scale factor and its derivatives. Consequently, different inflationary potentials, which result in distinct behaviors of the scale factor as per the Friedmann equation, lead to varying dynamics of  $\omega(\eta, \mathbf{k})$  and, consequently, diverse behaviors of  $v_{\mathbf{k}}(\eta)$ .

# Chapter 4

## Black Holes in the Early Universe

### 4.1 Misner's Chaotic Cosmology

The Mixmaster universe is a solution to Einstein's field equations in general relativity. Charles Misner studied this solution to gain a better understanding of the early universe's dynamics. His aim was to address the horizon problem by demonstrating that the early universe underwent a turbulent and oscillatory phase.

This model bears similarities to the closed FLRW universe. In both cases, spatial sections are positively curved and have a three-sphere topology ( $S^3$ ). However, in the FLRW universe, the  $S^3$  can only expand or contract, with the scale factor  $a(t)$  being the sole dynamic parameter. In contrast, the Mixmaster universe allows the  $S^3$  to not only expand or contract but also deform anisotropically. Its evolution is characterized by a scale factor  $a(t)$  and two shape parameters,  $\beta_+(t)$  and  $\beta_-(t)$ . These shape parameters describe deformations of the  $S^3$  that maintain its volume and a constant Ricci curvature scalar. Consequently, as the values of these three parameters,  $a$ ,  $\beta_+$ , and  $\beta_-$ , change, the universe retains homogeneity but not isotropy.

This model exhibits a complex dynamical structure. Misner demonstrated that the shape parameters  $\beta_+(t)$  and  $\beta_-(t)$  can be likened to coordinates of a point mass moving within a triangular potential with steep, rising walls and friction. By studying the motion of this point within the potential, Misner concluded that the physical universe would undergo expansion in certain directions and contraction in others, with the directions of expansion and contraction continually changing. Due to the roughly triangular nature of the potential, Misner suggested that the universe's evolution in this model is chaotic.

## 4.2 Gravitationally Collapsed Objects of Very Low Mass

The concept of primordial black holes (PBH) was first coined by Stephen Hawking in his 1971 paper [1] bearing the same title as this section. He postulated his theory on the basis of Misner's cosmology model. In his paper he wrote his theory aims to circumvent the need for assuming highly specialized initial conditions for the Universe to account for its current observed characteristics, such as its remarkable isotropy and the presence of galaxies. Instead, it posits that these features originally emerged from substantial random fluctuations occurring across all length scales during the early phases of the Universe.

During the early Universe, consider a comoving volume  $V$ . This volume would possess a gravitational binding energy approximately on the order of  $G\rho^2V^{5/3}$ , with  $\rho$  representing the density. Simultaneously, the kinetic energy associated with the matter's expansion within this volume would be roughly  $\rho V^{5/3}(\dot{V}/V)^2$ , and the potential energy stemming from relativistic pressure would be of the order of  $\rho c^2V$ . If  $V > (c^2/G\rho)^{3/2}$ , the potential energy can be safely disregarded when compared to the gravitational energy.

If the scenario involving substantial initial fluctuations is accurate, numerous such volumes must have existed in which the gravitational energy significantly surpassed the kinetic energy of expansion. These particular regions would not have continued expanding in tandem with the rest of the Universe; instead, they would have undergone gravitational collapse culminating to the formation of black holes. To prevent these collapsed regions from becoming entirely isolated, disconnected universes of their own, the mass within them must not be so immense as to separate them entirely from our Universe.

## 4.3 Theoretical Framework of Primordial Black Holes

The theory suggests black holes could have formed very early in the universe, shortly after the Big Bang, through various mechanisms. Here's a brief overview of the key theoretical ideas and mechanisms behind PBH formation:

### 1. Density Fluctuations during Inflation:

- Inflation is a theoretical period of rapid cosmic expansion in the early universe. Tiny quantum fluctuations during inflation can lead to variations in the energy density of the universe. Some regions with higher density fluctuations can collapse to form PBHs when the density exceeds a critical threshold.

### 2. Phase Transitions:

- During phase transitions in the early universe, such as those occurring in particle physics, localized regions of high energy density can form. If the conditions are right, these regions may lead to PBH formation.

### 3. **Critical Collapse:**

- In certain circumstances, if the matter density in a region exceeds a critical value, gravitational collapse can occur, forming PBHs. The formation of PBHs through critical collapse is sensitive to the initial conditions of the universe.

### 4. **Collapse of Cosmic Strings:**

- Cosmic strings are hypothetical one-dimensional topological defects that could have formed in the early universe. The intersections of cosmic strings might lead to the formation of PBHs.

### 5. **Primordial Gravitational Waves:**

- Gravitational waves generated during inflation can source density perturbations. If the amplitude of these waves is large enough, they can lead to PBH formation when they re-enter the horizon.

### 6. **Extended Inflaton Field:**

- Some models propose the existence of an extended inflaton field that can produce regions with higher density fluctuations, potentially leading to PBH formation.

### 7. **Large Extra Dimensions:**

- In models with large extra dimensions beyond the familiar three spatial dimensions, the modified gravitational physics can allow for the creation of PBHs at smaller scales.

### 8. **Axion Miniclusters:**

- The existence of axions, a type of hypothetical particle, could lead to the formation of dense clumps called axion miniclusters. Some of these miniclusters might undergo gravitational collapse to form PBHs.

### 9. **Non-Gaussian Density Fluctuations:**

- In addition to standard Gaussian density fluctuations, non-Gaussian fluctuations in the early universe can also lead to PBH formation if the non-Gaussianity is significant.

PBHs are intriguing because they provide a window into the early universe and can have implications for various cosmological and astrophysical phenomena, including dark matter, gravitational waves, and the structure of the early universe.

### 4.3.1 PBH Formation as a Causal Process

In an expanding spacetime, we often rely on the concept of the horizon scale, which plays a crucial role in understanding the causal properties of perturbations responsible for Primordial Black Hole (PBH) formation. The Hubble rate, denoted as  $H(t) \equiv \dot{a}(t)/a(t)$ , represents the rate of expansion of our universe and has dimensions of inverse length (or equivalently, time to the power of -1 in natural units). This naturally leads to the quantity  $H^{-1}$ , referred to as the Hubble horizon or the Hubble distance. It measures the distance that light can travel within one Hubble time, making it a suitable candidate for characterizing a time-dependent length scale governing the size of a causal patch in our universe.

To relate physical measurements to comoving ones, we use the scale factor  $a(t)$ . A valuable quantity in this context is the comoving Hubble horizon, denoted as  $(aH)^{-1}$ , especially when examining its time evolution. When expressed in terms of the second derivative of the scale factor, the time derivative of the comoving horizon can be represented as:

$$\frac{d}{dt} \left( \frac{1}{aH} \right) = -\frac{\ddot{a}}{a^2 H^2}. \quad (4.1)$$

As we know, during inflation, we have  $\ddot{a} > 0$ , resulting in the comoving horizon scale decreasing over time. Conversely, in a decelerating universe with  $\ddot{a} < 0$ , which occurs in the post-inflationary period before dark energy domination, this quantity increases with time. The fact that the comoving horizon decreases during an accelerated expansion is a key element in understanding inflation as a solution to the horizon problem in Hot Big Bang cosmology. It also provides a framework for the quantum mechanical origin of structures in our universe.

The time evolution of the comoving Hubble horizon is influenced by the background equation of state, denoted as  $w$ . It follows the relationship:

$$(aH)^{-1} \propto a^{(1+3w)/2}. \quad (4.2)$$

Therefore, during inflation  $w \simeq -1$  and  $(aH)^{-1} \propto a^{-1}$  while, during the subsequent phases of radiation dominated (RDU) and matter dominated universe (MDU), the comoving horizon evolves as  $(aH)^{-1} \propto a^1$  and  $(aH)^{-1} \propto a^{1/2}$  respectively.

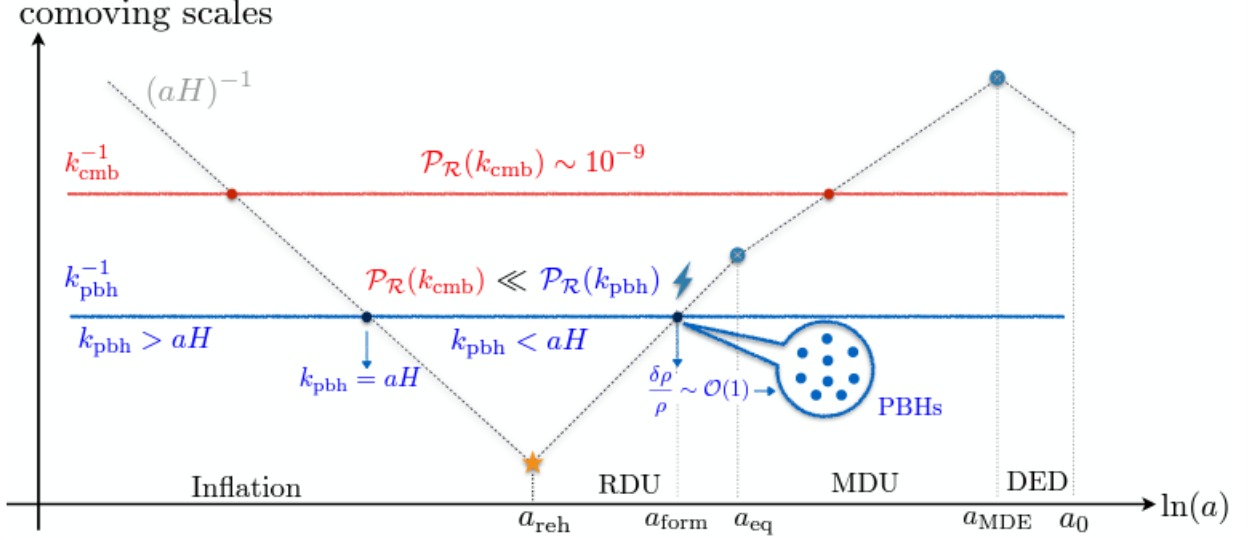


Figure 4.1: A schematic representation of the temporal evolution of curvature fluctuations  $\mathcal{R}$ , each marked by a comoving scale denoted as  $k^{-1}$ , concerning the comoving Hubble horizon (represented by dotted lines)  $(aH)^{-1}$  in the early universe. In the post-inflationary era, the symbol  $a_{\text{reh}}$  denotes the reheating time,  $a_{\text{eq}}$  refers to the time of matter-radiation equality,  $a_{\text{MDE}}$  represents the time of matter-dark energy equality, and  $a_0$  signifies the current value of the scale factor. The blue horizontal line in the diagram represents the comoving size of a typical small-scale perturbation responsible for Primordial Black Hole (PBH) formation. If the power spectrum associated with these modes is amplified during inflation, these perturbations can transfer their energy to density perturbations during the dominance of radiation. This energy transfer can lead to the initiation of PBH formation upon re-entry into the horizon when  $a = a_{\text{form}} \equiv a_f$ . [5]

The evolution of the comoving horizon concerning the natural logarithm of the scale factor  $\ln(a)$  is depicted in Figure 4.1. When analyzing the statistical properties of fluctuations in Fourier space, we often characterize a specific perturbation mode with a comoving length scale denoted as  $k^{-1}$ . This length scale is typically measured in units of megaparsecs (Mpc), equivalent to approximately  $3.26 \times 10^6$  light-years or roughly  $3.1 \times 10^{19}$  kilometers. Hence, a critical quantity for understanding perturbation behavior in the inflationary universe is the ratio of the wavelength of a given mode to the size of the comoving Hubble horizon, expressed as  $(aH)/k$ . Fluctuations with wavelengths larger than the comoving horizon fall into the category of super-horizon modes ( $k < aH$ ), while sub-horizon perturbations satisfy  $k > aH$ . Each mode crosses the horizon at  $k = aH$ .

As illustrated in Figure 4.1, a typical fluctuation with a comoving size of  $k^{-1}$  (repre-

sented by horizontal lines) initiates its existence well inside the horizon, often starting as a quantum fluctuation. Subsequently, it exits the horizon to become a super-horizon mode and eventually re-enters the comoving horizon during the post-inflationary era. Large-scale modes with smaller values of  $k$  exit the horizon at earlier times than small-scale modes, re-entering the horizon later during the post-inflationary period.

Indeed, aside from their role as the origin of the observed cosmic microwave background (CMB) anisotropies on large scales, the dynamics of curvature fluctuations  $\mathcal{R}$  might also contribute to the formation of Primordial Black Holes (PBHs). However, this requires specific "initial conditions" for cosmological fluctuations at small scales. To illustrate this, let's denote  $k = k_{\text{pbh}} \gg k_{\text{cmb}}$  as the comoving momentum associated with PBH formation. We assume that the curvature power spectrum at these small scales undergoes significant amplification, well above the level needed to match CMB observations:  $\mathcal{P}_{\mathcal{R}}(k_{\text{pbh}}) \gg \mathcal{P}_{\mathcal{R}}(k_{\text{cmb}}) \sim 10^{-9}$ .

Shortly after the end of inflation, i.e., after reheating, the modes associated with this amplification (e.g., modes with a comoving size of  $k_{\text{pbh}}^{-1}$ ) become the precursors of density perturbations in the radiation-dominated universe (RDU):

$$\mathcal{P}_{\mathcal{R}}(k_{\text{pbh}})^{1/2} \sim \frac{\delta\rho}{\rho}. \quad (4.3)$$

As the comoving Hubble scale expands concerning comoving scales in the RDU, the characteristic scale of these perturbations eventually becomes comparable to the comoving horizon at  $a = a_f$ , where  $k_{\text{pbh}} = (aH)_f$  (here, the subscript f indicates the time of PBH formation). At this juncture, gravitational interactions can trigger the collapse of overdense regions, provided these regions exhibit a sufficient overdensity exceeding a specific collapse threshold (more details are provided in the subsequent discussion).

## 4.4 Thorne's Hoop Conjecture

Kip Thorne introduced the hoop conjecture in 1972, suggesting that an object undergoing gravitational collapse transforms into a black hole only when it meets a specific criterion: a circular hoop with a precise critical circumference could be encompassed around the object and rotated about its diameter. In simpler terms, for a black hole to form, the object's entire mass must be compressed to the extent that it resides within a perfect sphere whose radius equals the Schwarzschild radius of that object. Failure to meet this condition means a black hole will not emerge. The formula expressing the critical circumference for this hypothetical hoop is as follows:

$$c = 2\pi r_s \quad (4.4)$$



Here,  $c$  represents the critical circumference, and  $r_s$  denotes the Schwarzschild radius of the object.

Thorne's investigations involved the gravitational effects on objects with various shapes, including spheres and infinitely long cylinders. He concluded that an object must undergo compression in all three dimensions before gravity induces the formation of a black hole. For cylindrical objects, the event horizon came into existence when the object could fit within the previously described hoop. While he couldn't provide mathematical proof for objects of all conceivable shapes at the time, he articulated this idea as the hoop conjecture.

#### 4.4.1 Threshold for Collapse

The first criterion regarding the collapse threshold for the formation of Primordial Black Holes (PBHs), denoted as  $\delta_c$ , hereafter, was established by B. Carr in 1975. Carr's approach employed a Jeans-type instability argument within the framework of Newtonian gravity. According to Carr's estimation, an over-density in the radiation-dominated universe (RDU) would undergo collapse upon re-entering the horizon if the fractional over-density of the perturbation exceeds the square of the sound speed associated with density perturbations, denoted as  $c_s^2$ . This sound speed represents the speed at which a pressure wave, caused by the over-density, can propagate from the center to the edge of a local fluctuation.

In the context of RDU, the speed of sound for perturbations satisfies  $c_s^2 = w = 1/3$ , where  $w$  is directly related to the Equation of State (EoS) during RDU. Essentially, this implies that a perturbation can collapse to give rise to PBHs if its over-density surpasses the pressure exerted by radiation pressure. When considering the effects of general relativity, a second analytical estimate was derived, obtaining  $\delta_c \approx 0.4$  during RDU. However, subsequent investigations in this area have revealed that the threshold depends on the initial profile of the curvature perturbation.

## 4.5 Mass and Collapse Function of PBH at Formation

The characteristic mass of Primordial Black Holes (PBHs) can be linked to the mass contained within the Hubble horizon at the time of their formation (denoted as  $a = a_f$ ) through an efficiency factor  $\gamma = 0.2$ :

$$M_{\text{pbh}}^{(f)} = \gamma M_H|_{a=a_f} = \gamma M_H^{(\text{eq})} \left( \frac{M_H^{(f)}}{M_H^{(\text{eq})}} \right) = \left( \frac{a_f}{a_{\text{eq}}} \right)^2 \gamma M_H^{(\text{eq})}. \quad (4.5)$$

Here,  $M_H(t) \equiv 4\pi\rho(t)/(3H(t)^3)$  represents the time-dependent horizon mass [5]. The subscripts  $f$  and  $eq$  signify quantities evaluated at the time of PBH formation and matter-radiation equality, respectively. During radiation-dominated universe (RDU), we utilize the standard relationships  $H^2 \propto \rho \propto a^{-4}$ . It's important to note that the horizon mass at the time of equality is approximately  $M_H^{(\text{eq})} \simeq 2.8 \times 10^{17} M_\odot$ . This equation informs us that PBHs, unlike astrophysical black holes, can potentially span a wide range of masses depending on their formation time relative to matter-radiation equality.

By using the time-dependent horizon mass as described above, we can establish a relationship between the mass of PBHs at formation and the characteristic size of the perturbations that exit the horizon during inflation, which are responsible for PBH formation. To achieve this, we first rewrite the PBH mass at formation as:

$$M_{\text{pbh}}^{(f)} = \left( \frac{\rho_f}{\rho_{\text{eq}}} \right)^{1/2} \left( \frac{H_{\text{eq}}}{H_f} \right)^2 \gamma M_H^{(\text{eq})}. \quad (4.6)$$

Utilizing the conservation of entropy  $g_s(T)T^3 a^3 = \text{constant}$  and the scaling property of energy density with respect to the temperature of the plasma during RDU  $\rho \propto g_*(T)T^4$ , the previous equation can be re-expressed as:

$$M_{\text{pbh}}^{(f)}(k_{\text{pbh}}) = \left( \frac{g_*(T_f)}{g_*(T_{\text{eq}})} \right)^{1/2} \left( \frac{g_s(T_{\text{eq}})}{g_s(T_f)} \right)^{2/3} \left( \frac{k_{\text{eq}}}{k_{\text{pbh}}} \right)^2 \gamma M_H^{(\text{eq})}. \quad (4.7)$$

Expanding upon the above equation, we can also derive an approximate relationship between the PBH mass at formation and the number of e-folds, denoted as  $N_{\text{pbh}}$ , during which the modes that give rise to PBHs exit the horizon during inflation. To do this, we first note that  $k_{\text{pbh}}/k_{\text{cmb}} = (aH)_{\text{pbh}}/(aH)_{\text{cmb}}$ , where the values of the Hubble rate and scale factor should be evaluated at the scales of horizon exit during inflation (as depicted in Figure 4.1).

Assuming that the slow-roll parameter  $\epsilon \equiv -\dot{H}/H^2 \ll 1$  remains roughly constant between the horizon-exit time of modes associated with the Cosmic Microwave Background (CMB) and PBH formation, we can relate the Hubble rate and scale factor as follows:  $H_{\text{pbh}} = H_{\text{cmb}} e^{-\epsilon(N_{\text{pbh}} - N_{\text{cmb}})}$  and  $a_{\text{pbh}} = a_{\text{cmb}} e^{N_{\text{pbh}} - N_{\text{cmb}}}$ . Here,  $N_{\text{pbh}} > N_{\text{cmb}}$  so that we count e-folds forward in time concerning the horizon exit of the CMB mode.

Using these two relations, we find  $k_{\text{pbh}}/k_{\text{cmb}} \simeq e^{(N_{\text{pbh}} - N_{\text{cmb}})(1 - \epsilon)}$ . When this is inserted into mass equation, assuming  $k_{\text{cmb}} = 0.002 \text{Mpc}^{-1}$ , we obtain:

$$M_{\text{pbh}}^{(f)}(N_{\text{pbh}}) \approx 7.7 \times 10^{17} M_{\odot} e^{-2(N_{\text{pbh}} - N_{\text{cmb}})(1-\epsilon)} \left(\frac{\gamma}{0.2}\right) \left(\frac{g_*(T_f)}{106.75}\right)^{-1/6}. \quad (4.8)$$

It's worth noting that modes exiting the horizon significantly later than CMB scales, denoted as  $N_{\text{pbh}} - N_{\text{cmb}} \gg 1$ , will have a substantial reduction in the exponential term in the equation above. **Consequently, this reduction can lead to smaller PBH masses.**

The abundance of PBHs at their formation can also be seen as the fraction, denoted as  $\beta$ , of local regions within the universe that possess a density exceeding a specific threshold. The conventional approach for estimating  $\beta$  relies on the Press-Schechter model of gravitational collapse, a widely employed concept in the field of large-scale structure formation. This model is expressed as follows:

$$\beta \equiv \frac{\rho_{\text{pbh}}}{\rho} \Big|_{a=a_f} \equiv \int_{\Delta_c}^{\infty} P(\delta) d\delta \quad (4.9)$$

In this equation,  $\beta$  represents the fraction of regions in the universe where the density exceeds a certain threshold, and it is evaluated at the time of PBH formation ( $a = a_f$ ). The integral encompasses values of the density contrast  $\delta$  ranging from  $\Delta_c$  to infinity, with  $P(\delta)$  representing the probability distribution function associated with  $\delta$ . In this context,  $P(\delta)$  corresponds to the probability distribution function (PDF), which characterizes the likelihood of a given fluctuation possessing a density contrast  $\delta$ . It is assumed that a perturbation will collapse to form a black hole if its amplitude surpasses a critical value denoted as  $\Delta_c$ . It's important to note that  $\Delta_c$  represents the critical density contrast, and generally, it should not be confused with the threshold, where  $\Delta_c \neq \delta_c$ . The latter,  $\delta_c$ , can be defined as the peak value of the compaction function and is related to an averaged density contrast.

# Chapter 5

## Quantum Fields in Curved Space-Time

In our exploration of characterizing classical geometry from a quantum perspective, it is essential for us to consider the background geometry in question. This prompts us to expand our quantum field theory to include curved space-times, ensuring that we encompass all the quantum characteristics of matter as sources. This approach involves assuming that the expectation values of relevant quantities closely align with classical dynamics, providing a systematic way to account for quantum effects within a curved space-time framework.

### 5.1 The Background Field Method

In a fully quantum description of the Universe, it is expected that all measurable quantities can be expressed as the expected values of specific operators, denoted as  $\hat{O}$ , acting on a quantum state  $|\psi\rangle$ . However, because many of these observables currently appear to satisfy classical equations quite accurately, the quantum state  $|\psi\rangle$  must be chosen in a way that ensures:

$$\langle\psi|\hat{O}|\psi\rangle \simeq O_{\text{cl}}, \quad (5.1)$$

where  $O_{\text{cl}}$  complies with the classical equations that  $\hat{O}$  adheres to as an operator.

This concept underlies the background field method. Since the state  $|\psi\rangle$  is not precisely known, it is assumed that all observables can be expressed as:

$$O = O_{\text{cl}} + o, \quad (5.2)$$

where the "perturbation"  $o$  is considered "small," and this is the only quantity treated as an operator in the semi-classical quantum theory:

$$O \rightarrow O_{\text{cl}} + \hat{o}. \quad (5.3)$$

Once we embrace this separation, the natural progression is to apply it to all fields, including the metric:

$$g_{\mu\nu} \rightarrow g_{\mu\nu}^{\text{cl}} + \epsilon \hat{h}_{\mu\nu}, \quad (5.4)$$

Additionally, the matter fields can be described as follows:

$$\phi \rightarrow \psi_{\text{cl}} + \epsilon \hat{\phi} \quad (5.5)$$

Here, we introduce the parameter  $\epsilon$  to formally account for the expansion, and it is worth noting that one might intuitively relate  $\epsilon$  to  $\hbar$ .

Another assumption we can make is that the classical components of both the metric and matter fields satisfy the Einstein field equations. This assumption leads to the emergence of a classical space-time manifold denoted as  $(\mathcal{M}, \mathbf{g}_{\text{cl}})$  on which we can analyze the quantum fields  $\hat{h}_{\mu\nu}$  and  $\hat{\phi}$ . It is important to emphasize that, within this approximation, the gravitational perturbations represented by  $h_{\mu\nu}$  behave simply as a spin 2 field. Specifically, they do not directly influence the causal structure determined by  $g_{\mu\nu}^{\text{cl}}$  but instead interact with other matter fields through terms that can be derived by expanding the matter action.

### 5.1.1 The Vacuum Ambiguity

Due to the background field method, since the background is chosen independent of the quantum states, the vacuum becomes ambiguous.

The vacuum ambiguity in quantum field theory (QFT) in curved spacetime arises from the fundamental tension between the principles of quantum mechanics and the geometry of curved spacetime in the context of general relativity. Here's why this ambiguity exists:

1. **Local vs. Global Effects:** In flat spacetime (Minkowski spacetime), the vacuum state is well-defined and uniform throughout space. However, in curved spacetime, due to the equivalence principle of general relativity, there are no globally inertial frames of reference. This means that what is considered "vacuum" can differ from one region of spacetime to another, leading to local variations in the vacuum state.
2. **Quantum Field Fluctuations:** In quantum field theory, vacuum fluctuations are an inherent part of the quantum description of fields. Even in the absence of external forces or particles, quantum fields exhibit fluctuations at every point in spacetime. These fluctuations can be thought of as particles and antiparticles spontaneously appearing and

annihilating. In curved spacetime, these fluctuations are influenced by the curvature itself.

3. Observer Dependence: Observers in different states of motion or located at different positions in curved spacetime can make different observations regarding the number and properties of particles in the vacuum state. This is a consequence of the principle of locality in QFT, which states that measurements at one spacetime point should not instantaneously affect measurements at a distant point. The observer's motion or location can affect their perception of particles due to the way spacetime curvature influences the behavior of quantum fields.

### 5.1.2 Particle Creation in a Gravitational Background

In this section we review the fundamentals of particle creation that arises due to a background gravitational field and is one of the key elements to this thesis.

Let's consider a spacetime that exhibits asymptotic flatness both in the past and in the future, but deviates from flatness in the intermediate region. In the past, we have a set of positive frequency solutions denoted as  $\{f_j\}$  (referred to as the "in-region"), and in the future, we have another set of positive frequency solutions denoted as  $\{F_j\}$  (referred to as the "out-region"). We can choose these sets of solutions to be orthonormal, meaning [4]:

We define the inner product of a pair of these solutions of generally covariant Klein-Gordon equations,

$$(f_1, f_2) = i \int_{\Sigma} (f_2^* \overleftrightarrow{\partial}_{\mu} f_1) d\Sigma^{\mu} \quad (5.6)$$

where  $d\Sigma^{\mu} = d\Sigma n^{\mu}$  with  $d\Sigma$  being the volume element in a given spacelike hypersurface, and  $n^{\mu}$  being the timelike unit vector normal to this hypersurface.

- The inner product of  $f_j$  and  $f_{j'}$  is equal to the inner product of  $F_j$  and  $F_{j'}$  and both are equal to  $\delta_{jj'}$ .
- The inner product of the complex conjugates of  $f_j$  and  $f_{j'}$  is equal to the inner product of the complex conjugates of  $F_j$  and  $F_{j'}$ , both of which are equal to  $-\delta_{jj'}$ .
- The inner product between  $f_j$  and  $f_{j'}^*$ , as well as between  $F_j$  and  $F_{j'}^*$ , is equal to zero.

Even though these functions are primarily defined by their behavior in different regions, they are solutions of the wave equation across the entire spacetime. We can express the in-region modes using the out-region modes as follows:

$$f_j = \sum_k (\alpha_{jk} F_k + \beta_{jk} F_k^*) \quad (5.7)$$

When we insert this expansion into the orthogonality relations it leads to the following conditions:

$$\sum_k (\alpha_{jk} \alpha_{j'k}^* - \beta_{jk} \beta_{j'k}^*) = \delta_{jj'} \quad (5.8)$$

This equation establishes the relationship between the coefficients  $\alpha_{jk}$  and  $\beta_{jk}$  that relate the in-modes and out-modes while preserving orthonormality. Furthermore,

$$\sum_k (\alpha_{jk} \alpha_{j'k} - \beta_{jk} \beta_{j'k}) = 0 \quad (5.9)$$

The inverse expansion takes the form of

$$F_k = \sum_j (\alpha_{jk}^* f_j - \beta_{jk} f_j^*) \quad (5.10)$$

The field operator, denoted as  $\varphi$ , can be expressed using either the set  $\{f_j\}$  or  $\{F_j\}$  as follows:

$$\varphi = \sum_j (a_j f_j + a_j^\dagger f_j^*) = \sum_j (b_j F_j + b_j^\dagger F_j^*) \quad (5.11)$$

Here,  $a_j$  and  $a_j^\dagger$  are the annihilation and creation operators, respectively, within the in-region, while  $b_j$  and  $b_j^\dagger$  are their counterparts in the out-region. The in-vacuum state is defined as  $a_j |0\rangle_{\text{in}} = 0$  for all  $j$ , representing the absence of particles initially. Similarly, the out-vacuum state is defined as  $b_j |0\rangle_{\text{out}} = 0$  for all  $j$ , indicating the absence of particles at later times. It's worth noting that  $a_j = (\varphi, f_j)$  and  $b_j = (\varphi, F_j)$ , allowing us to express the two sets of creation and annihilation operators in terms of each other as:

$$a_j = \sum_k (\alpha_{jk}^* b_k - \beta_{jk}^* b_k^\dagger) \quad (5.12)$$

or

$$b_k = \sum_j (\alpha_{jk} a_j + \beta_{jk}^* a_j^\dagger) \quad (5.13)$$

This represents a Bogolubov transformation, with the coefficients  $\alpha_{jk}$  and  $\beta_{jk}$  known as the Bogolubov coefficients.

Now, let's explore the physical phenomenon of particle creation due to a time-dependent gravitational field. We assume that no particles were present before the gravitational field was activated. When using the Heisenberg picture to describe quantum dynamics,

$|0\rangle_{\text{in}}$  represents the system's state at all times. However, the physical number operator that counts particles in the out-region is  $N_k = b_k^\dagger b_k$ . Consequently, the average number of particles created in mode  $k$  is given by:

$$\langle N_k \rangle = {}_{\text{in}} \langle 0 | b_k^\dagger b_k | 0 \rangle_{\text{in}} = \sum_j |\beta_{jk}|^2 \quad (5.14)$$

If any of the  $\beta_{jk}$  coefficients are non-zero, indicating a mixing of positive and negative frequency solutions, particles are indeed created by the gravitational field.

## 5.2 Bogolubov Transformation of Squeezed States

In this section, we will provide a concise overview of quantized fields on a flat Friedmann-Lemaitre-Robertson-Walker (FLRW) background [6]. Let's start by considering a real massless scalar field denoted as  $\phi$ . The dynamics of this field are described by the following action, denoted as  $S$ :

$$S = \frac{1}{2} \int d^4x \sqrt{-g} \partial^\mu \phi \partial_\mu \phi \quad (5.15)$$

In this expression,  $\mu$  takes values from 0 to 3, and we use natural units where  $c$  and  $\hbar$  are set to 1. Additionally, we adhere to the Landau-Lifshitz sign conventions.

The spacetime metric for this scenario is given by:

$$ds^2 = dt^2 - a^2(t) \delta_{ij} dx^i dx^j \quad (5.16)$$

Here,  $i$  and  $j$  run from 1 to 3.

Now, let's briefly outline how the dynamics of this system lead to the emergence of squeezed states. We start by expressing the classical Hamiltonian, denoted as  $H$ , in terms of the field  $y$  defined as  $y \equiv a\phi$  and the conformal time  $\eta$  defined as  $\eta = \int \frac{dt}{a(t)}$ . The result can be written as follows:

$$H = \int d^3\mathbf{x} \mathcal{H}(y, p, \partial_i y, t) \quad (5.17)$$

$$= \frac{1}{2} \int d^3\mathbf{k} \left[ p(\mathbf{k}) p^*(\mathbf{k}) + k^2 y(\mathbf{k}) y^*(\mathbf{k}) + \frac{a'}{a} (y(\mathbf{k}) p^*(\mathbf{k}) + p(\mathbf{k}) y^*(\mathbf{k})) \right] \quad (5.18)$$

where

$$p \equiv \frac{\partial \mathcal{L}(y, y')}{\partial y'} = y' - \frac{a'}{a} y \quad (5.19)$$



and a prime denotes differentiation with respect to the conformal time. We use the following Fourier transform convention:  $\Phi(\mathbf{k}) \equiv (2\pi)^{-3/2} \int \Phi(\mathbf{r}) e^{-i\mathbf{k}\mathbf{r}} d^3\mathbf{r}$  for both functions and operators. To simplify notation, we sometimes write  $y(\mathbf{k}), a(\mathbf{k}), \dots$  instead of  $y(\mathbf{k}, \eta), a(\mathbf{k}, \eta), \dots$ , even though the Fourier transforms depend on time in the Heisenberg representation. Since the field  $y$  is real, we have  $y(\mathbf{k}) = y^*(-\mathbf{k})$ , or  $y^\dagger(-\mathbf{k})$  for operators. This means that any classical field configuration is fully described by giving the Fourier transforms in half Fourier space. However, in the quantum case, the entire Fourier space must be used if a quantum state of the field is not invariant under the reflection  $\mathbf{k} \rightarrow -\mathbf{k}$ . Fortunately, for the vacuum initial state we will use below, this complication does not arise. The Fourier transforms satisfy the equation:

$$y''(\mathbf{k}) + \left(k^2 - \frac{a''}{a}\right) y(\mathbf{k}) = 0 \quad (5.20)$$

When the field  $y$  is quantized, the Hamiltonian becomes:

$$H = \int \frac{d^3\mathbf{k}}{2} \left[ k (a(\mathbf{k})a^\dagger(\mathbf{k}) + a^\dagger(\mathbf{k})a(\mathbf{k})) + i \frac{a'}{a} (a^\dagger(\mathbf{k})a^\dagger(-\mathbf{k}) - a(\mathbf{k})a(-\mathbf{k})) \right] \quad (5.21)$$

The time-dependent (in the Heisenberg representation) operator  $a(\mathbf{k})$  is defined as usual:

$$a(\mathbf{k}) = \frac{1}{\sqrt{2}} \left( \sqrt{k} y(\mathbf{k}) + i \frac{1}{\sqrt{k}} p(\mathbf{k}) \right) \quad (5.22)$$

so that

$$y(\mathbf{k}) = \frac{a(\mathbf{k}) + a^\dagger(-\mathbf{k})}{\sqrt{2k}}, \quad p(\mathbf{k}) = -i\sqrt{\frac{k}{2}} (a(\mathbf{k}) - a^\dagger(-\mathbf{k})) \quad (5.23)$$

The canonical commutation relations are given by:

$$[y(\mathbf{x}, \eta), p(\mathbf{x}', \eta)] = i\delta^{(3)}(\mathbf{x} - \mathbf{x}') \quad (5.24)$$

These relations imply the following commutation relations:

$$[y(\mathbf{k}, \eta), p^\dagger(\mathbf{k}', \eta)] = i\delta^{(3)}(\mathbf{k} - \mathbf{k}'), \quad [a(\mathbf{k}, \eta), a^\dagger(\mathbf{k}', \eta)] = \delta^{(3)}(\mathbf{k} - \mathbf{k}'). \quad (5.25)$$

The final term in the integrand of the Hamiltonian is responsible for the phenomenon of squeezing. First, let's examine how it influences the time evolution of the system. We have:

$$\begin{pmatrix} a'(\mathbf{k}) \\ (a^\dagger(-\mathbf{k}))' \end{pmatrix} = \begin{pmatrix} -ik & \frac{a'}{a} \\ \frac{a'}{a} & ik \end{pmatrix} \begin{pmatrix} a(\mathbf{k}) \\ a^\dagger(-\mathbf{k}) \end{pmatrix} \quad (5.26)$$

Clearly, the general solutions to these two coupled equations are:

$$\begin{aligned} a(\mathbf{k}, \eta) &= u_k(\eta)a(\mathbf{k}, \eta_0) + v_k(\eta)a^\dagger(-\mathbf{k}, \eta_0), \\ a^\dagger(-\mathbf{k}, \eta) &= u_k^*(\eta)a^\dagger(-\mathbf{k}, \eta_0) + v_k^*(\eta)a(\mathbf{k}, \eta_0). \end{aligned} \quad (5.27)$$

This is essentially a Bogolubov transformation. The coupled equations can be interpreted as describing the time evolution of the creation and annihilation operators in the Heisenberg representation, or as a definition of explicitly time-dependent operators in the Schrödinger representation. The commutation relations remain unchanged under the unitary time evolution, leading to the constraint:

$$|u_k(\eta)|^2 - |v_k(\eta)|^2 = 1, \quad (5.28)$$

which permits the following standard parameterization of the functions  $u_k$  and  $v_k$ :

$$\begin{aligned} u_k(\eta) &= e^{-i\theta_k(\eta)} \cosh r_k(\eta), \\ v_k(\eta) &= e^{i(\theta_k(\eta)+2\varphi_k(\eta))} \sinh r_k(\eta). \end{aligned} \quad (5.29)$$

In this context, we have the squeezing parameter denoted as  $r_k$ , the squeezing angle referred to as  $\varphi_k$ , and the phase represented by  $\theta_k$ .

The relationship between these quantities and those introduced in the  $\alpha - \beta$  formalism is as follows:

$$u_k = \alpha_k e^{-ik\eta}, \quad v_k^* = \beta_k e^{ik\eta}. \quad (5.30)$$

### 5.2.1 The Unruh-DeWitt Particle Detector

As we have seen before, in many problems of interest, spacetime can be approximated as asymptotically Minkowskian in both the distant past and future. In such scenarios, selecting the 'natural' Minkowskian vacuum holds a well-defined physical significance. It represents the absence of particles according to all inertial observers in these remote regions, aligning with the commonly accepted notion of a vacuum.

Whether a particular spacetime can be considered a suitable "in" or "out" region may also depend on the specific quantum field under consideration. For instance, in the case of massless, conformally coupled fields, even a conformally flat spacetime, even if not static, can be a viable candidate for such regions. This allows for flexibility in choosing the appropriate spacetime framework for quantum field analysis.

To illustrate these concepts, we will examine a particle detector model introduced by Unruh (1976) and DeWitt (1979) [7]. This model features an idealized point particle

with internal energy levels labeled by the energy parameter  $E$ . The particle is coupled to a scalar field  $\phi$  through a monopole interaction. Our analysis takes place within four-dimensional Minkowski space.

Let's consider the scenario in which the particle detector moves along a world line defined by the functions  $x^\mu(\tau)$ , where  $\tau$  represents the detector's proper time. The interaction between the detector and the field is governed by an interaction Lagrangian denoted as  $cm(\tau)\phi[x(\tau)]$ . Here,  $c$  serves as a small coupling constant, and  $m$  represents the detector's monopole moment operator. We assume that the field  $\phi$  is initially in the vacuum state denoted as  $|0_M\rangle$ , where the subscript  $M$  indicates the 'Minkowski vacuum.'

For a general trajectory of the detector, it will not remain in its ground state  $E_0$ . Instead, it will undergo a transition to an excited state with energy  $E$  greater than  $E_0$ . Simultaneously, the field will also transition to an excited state represented by  $|\psi\rangle$ . When the coupling constant  $c$  is sufficiently small, we can compute the amplitude for this transition using first-order perturbation theory:

$$ic \left\langle E, \psi \left| \int_{-\infty}^{\infty} m(\tau)\phi[x(\tau)]d\tau \right| 0_M, E_0 \right\rangle \quad (5.31)$$

Utilizing the equation describing the time evolution of  $m(\tau)$  as:

$$m(\tau) = e^{iH_0t} m(0) e^{-iH_0\tau} \quad (5.32)$$

where  $H_0|E\rangle = E|E\rangle$ , the transition amplitude mentioned above can be factored, resulting in:

$$ic \langle E|m(0)|E_0\rangle \int_{-\infty}^{\infty} e^{i(E-E_0)\tau} \langle \psi|\phi(x)|0_M\rangle d\tau \quad (5.33)$$

When  $\phi$  is expanded in terms of standard Minkowski plane wave modes, it becomes evident that, at this order of perturbation theory, transitions can only occur to the state  $|\psi\rangle = |1_k\rangle$ , which contains one quantum with frequency  $\omega = (|\mathbf{k}|^2 + m^2)^{1/2}$  for some  $\mathbf{k}$ . Then, using the continuum normalization, we find:

$$\begin{aligned} \langle 1_{\mathbf{k}}|\phi(x)|0_M\rangle &= \int d^3k' (16\pi^3\omega')^{-1} \langle 1_{\mathbf{k}}|a_{\mathbf{k}'}^\dagger|0_M\rangle e^{-i\mathbf{k}'\cdot\mathbf{x}+i\omega't} \\ &= (16\pi^3\omega)^{-1} e^{-i\mathbf{k}\cdot\mathbf{x}+i\omega t} \end{aligned} \quad (5.34)$$

## 5.3 Semi-classicality and Decoherence of Momentum Modes

Let's proceed to define the field modes as  $f_k(\eta)$ , with  $\text{Re } f_k$  denoted as  $f_{k1}$  and  $\text{Im } f_k$  as  $f_{k2}$ . These modes satisfy the initial condition  $f_k(\eta_0) = 1/\sqrt{2k}$ . We will adopt a similar notation for the quantities  $p$  and  $y$ . Specifically:

$$\begin{aligned} y(\mathbf{k}) &\equiv f_k(\eta)a(\mathbf{k}, \eta_0) + f_k^*(\eta)a^\dagger(-\mathbf{k}, \eta_0) \\ &= \sqrt{2k}f_{k1}(\eta)y(\mathbf{k}, \eta_0) - \sqrt{\frac{2}{k}}f_{k2}(\eta)p(\mathbf{k}, \eta_0) \end{aligned} \quad (5.35)$$

and for the momentum modes  $g_k(\eta)$ , where  $g_k(\eta_0) = \sqrt{\frac{k}{2}}$ :

$$\begin{aligned} p(\mathbf{k}) &\equiv -i [g_k(\eta)a(\mathbf{k}, \eta_0) - g_k^*(\eta)a^\dagger(-\mathbf{k}, \eta_0)] \\ &= \sqrt{\frac{2}{k}}g_{k1}(\eta)p(\mathbf{k}, \eta_0) + \sqrt{2k}g_{k2}(\eta)y(\mathbf{k}, \eta_0). \end{aligned} \quad (5.36)$$

It's important to note that the modes  $f_k$  satisfy the Euler-Lagrange equation. Additionally, we have [6]:

$$\begin{aligned} f_k &= \frac{u_k + v_k^*}{\sqrt{2k}}, \quad |f_k|^2 = \frac{1}{2k} (\cosh 2r_k + \cos 2\varphi_k \sinh 2r_k), \\ g_k &= \sqrt{\frac{k}{2}}(u_k - v_k^*) = i \left( f_k' - \frac{a'}{a} f_k \right). \end{aligned} \quad (5.37)$$

In the context of inflationary theories, the initial perturbations are generated by vacuum quantum fluctuations of a real scalar field, and the power spectrum of these quantum fluctuations is represented by  $|f_k|^2$ . Let's focus on a crucial example involving a massless real scalar field in (quasi) de Sitter space. In this scenario, the expressions are as follows :

$$\sqrt{2k}f_k = e^{-ik\eta} \left( 1 - \frac{i}{k\eta} \right), \quad \sqrt{\frac{2}{k}}g_k = e^{-ik\eta}, \quad \text{where } \eta \equiv -\frac{1}{aH} < 0. \quad (5.38)$$

Here, the parameter  $\eta$  is defined as the negative reciprocal of the product of the scale factor  $a$  and the Hubble parameter  $H$ .

### 5.3.1 Long-wave Mode Behaviour

The fundamental process behind the emergence of the Bogolubov transformation and the extreme squeezing in the Universe is well-established and primarily stems from the

expansion of the Universe, which does not necessarily require inflation, and the presence of the Hubble radius denoted as  $R_H \equiv H^{-1} = \frac{a^2}{a'}$ .

For modes with wavelengths much larger than the Hubble radius, which can be expressed as  $kR_H \ll a$ , the general solution of the Mukhanov-Sasaki equation takes the following form in terms of the mode functions  $f_k$ , with  $y(\mathbf{k})$  expressed through  $f_k$ :

$$f_k = C_1(\mathbf{k})a + C_2(\mathbf{k})a \int_{\infty}^{\eta} \frac{d\eta'}{a^2(\eta')} \quad (5.39)$$

$C_1(\mathbf{k})$  can be made real by applying a phase rotation. Then, the normalization condition leads to the relation:

$$C_1 \text{Im} C_2 = -\frac{1}{2} \quad (5.40)$$

The first term in the general solution represents the quasi-isotropic mode, also referred to as the growing mode. This mode corresponds to a field  $\phi$  with a constant value. A similar behavior is observed in the dominant component of scalar (adiabatic) metric perturbations within the synchronous gauge for any arbitrary scale factor  $a(\eta)$ , as well as in the gravitational potential  $\Phi$  during stages of power-law expansion. The term "quasi-isotropic" implies that this mode does not disrupt the isotropic expansion of the universe in its early stages. The second term in the equation represents the decaying mode.

In the context of inflationary models, if we compare with the prior forms of the field modes, we find the following relations [6]:

$$C_1 = \frac{H_k}{\sqrt{2k^3}}, \quad C_2 = -\frac{ik^{3/2}}{\sqrt{2}H_k} \quad (5.41)$$

These relations are consistent with the general solution and the normalization condition, where  $H_k$  represents the value of the slowly varying Hubble parameter  $H$  at the moment of the first Hubble radius crossing, denoted as  $\eta_1$  (with  $\eta_1 < 0$  and  $|\eta_1(k)| = k^{-1}$ ).

# Chapter 6

## Corpuscular Theory of Gravity

The corpuscular theory of gravity, also known as the particle theory of gravity, is an early scientific hypothesis that attempted to explain the force of gravity in terms of particles or corpuscles. This theory was developed in contrast to the more famous theory of gravitation put forth by Sir Isaac Newton, which described gravity as an attractive force between masses. The corpuscular theory sought to provide an alternative explanation for the gravitational phenomenon.

### 6.1 Black Hole's Quantum N-Portrait

It is essential to grasp the concept of classicality from a quantum perspective. Black holes are typically described using classical solutions and geometry, but the underlying nature of the universe is fundamentally quantum. In our framework, we interpret any classical entity as a quantum bound state characterized by a high occupation number, denoted as  $N \gg 1$  [8]. Such bound states can exhibit various characteristics, including different relevant wavelengths and diverse oscillation patterns and frequencies.

As it is demonstrated in various literature, among the diverse range of macroscopic objects, black holes and solitons emerge as the simplest ones. Their physics can be effectively captured by a single quantum characteristic, which is the value of  $N$ . It is noteworthy that all the distinctive properties of black holes can be comprehended in terms of this solitary parameter,  $N$ . This numerical quantity serves as our primary metric for quantifying classicality in the context of this framework.

The idea [3] is to form a graviton wave-packet made of as many gravitons as possible, let us say  $N$ , with a typical wavelength  $\lambda_G \gg \ell_P$ . Clearly, since

$$\alpha_G = \frac{\hbar G_N}{\lambda_G^2} = \frac{\ell_P^2}{\lambda_G^2} \ll 1, \quad (6.1)$$

where  $\alpha_G$  is the effective coupling of  $N$  gravitons.

In this scenario, a cluster of gravitons will exhibit very weak interactions among themselves. However, when multiple gravitons come together, each one begins to experience a collective potential generated by the other  $N - 1$  constituents of the system.

The collective binding potential perceived by each graviton, at a first-order approximation, can be estimated as  $U \approx -\alpha_G N \hbar / \lambda_G$ , assuming a distance of approximately  $r \approx \lambda_G$ . Additionally, each graviton possesses kinetic energy given by  $K \approx |\mathbf{p}_G| \approx \hbar / \lambda_G$ . Thus, to create a bound state from these  $N$  gravitons, one simply needs to ensure that the energy balance  $K + U \approx 0$  (the marginally bound condition) is met for each graviton. This requirement implies

$$\alpha_G N \approx 1,$$

which corresponds to a classicalization scaling.

## 6.2 Corpuscular Black Holes

In an asymptotically flat space, the Hamiltonian constraint takes the form given by equations [9]:

$$H \equiv H_B + H_G = M, \tag{6.2}$$

Here,  $H_B$  and  $H_G$  represent the (super)Hamiltonians of matter and gravity, respectively. They are obtained by varying the action with respect to the lapse function, and  $M$  arises from boundary terms. For instance, one can consider configurations with a constant  $R = R_s$  to represent stable stars (where the Hamiltonian constraint leads to the Tolman-Oppenheimer-Volkov equation). Alternatively, as  $R$  decreases to form a black hole with a size equal to the Schwarzschild gravitational radius, given by:

$$R_H = 2\ell_p \frac{M}{m_p}. \tag{6.3}$$

If we idealize the system with  $N_B$  baryons initially very far apart, the total energy is simply the baryonic rest mass:

$$H = E_B \equiv \mu N_B \simeq M. \tag{6.4}$$

As the radius  $R$  shrinks, the baryon energy decreases due to the negative interaction potential energy  $U_{BG}$  between baryons mediated by gravitons and gains kinetic energy  $K_B$ , resulting in:

$$E_B(R) = M + K_B(R) + U_{BG}(R) + U_{BB}(R). \tag{6.5}$$

Here,  $U_{\text{BB}} \geq 0$  represents an additional repulsive interaction among baryons, providing the pressure required for a static configuration at a given finite value of  $R = R_s$  (where  $K_{\text{B}}(R_s) = 0$ ). In a classical model, this equals the total energy of the system, the ADM mass  $M$ , leading to the classical equation of motion:

$$K_{\text{B}}(R) + U_{\text{BG}}(R) + U_{\text{BB}}(R) = 0. \quad (6.6)$$

However, considering the quantum nature of baryons and the gravitational interaction, we must also account for quantum effects. Starting with a simple estimate of the total baryon gravitational potential energy for a static configuration obtained from Newtonian physics:

$$U_{\text{BG}}(R) \simeq N_{\text{B}}\mu\phi_{\text{N}}(R) \simeq -\frac{M^2\ell_{\text{p}}}{m_{\text{p}}R}, \quad (6.7)$$

where  $\phi_{\text{N}}$  satisfies the Poisson equation:

$$\Delta\phi_{\text{N}} = \ell_{\text{p}}\frac{M}{m_{\text{p}}}j(r), \quad (6.8)$$

with a static source profile ensuring  $\int_0^R r^2 dr j(r) = 1$ . In the quantum theory, the field can be described using a coherent state of virtual gravitons, akin to how a coherent state of virtual photons reproduces the Coulomb field around a static charge. This is expressed as:

$$k^2\phi_{\text{N}}(k) = -\frac{M}{m_{\text{p}}}j(k), \quad (6.9)$$

Where  $k$  is a dimensionless wave number, and  $\hat{\phi}_k \simeq (\hat{g}_k + \hat{g}_{-k}^\dagger) / \sqrt{k}$ . The coherent state is an eigenstate of the annihilation operators:

$$\hat{g}_k|g\rangle = g(k)|g\rangle, \quad (6.10)$$

And one can choose:

$$g(k) \simeq -\frac{Mj(k)}{m_{\text{p}}k^{3/2}}, \quad (6.11)$$

which reproduces the classical field. The expectation value of the graviton number can be approximated as:

$$N_{\text{G}} \simeq \frac{M^2}{m_{\text{p}}^2} \int dk \frac{j^2(k)}{k} \sim \frac{R_{\text{H}}^2}{\ell_{\text{p}}^2}. \quad (6.12)$$

This result resembles Bekenstein's area law and holds independently of the size  $R$  of the matter source.



### 6.3 Black Holes as Bose-Einstein Condensates

Consequently, when considering a black hole with an ADM mass of  $M$ , we can conceptualize it in this "corpuscular framework" as a self-sustained bound state, or a Bose-Einstein condensate [10], consisting of  $N$  gravitons with typical wavelengths around  $\lambda_G \approx R_H$  and mutual interaction strength  $\alpha_G = 1/N$ . Since  $\alpha_G = \ell_P^2/\lambda_G^2$ , this implies  $\lambda_G \approx \sqrt{N}\ell_P$ , leading to  $M \approx \sqrt{N}m_P$ . When these relationships are considered together, they give rise to the so-called scaling laws for corpuscular black holes:

$$M = \sqrt{N}m_P, \quad \lambda_G \approx \sqrt{N}\ell_P, \quad \alpha_G \approx \frac{1}{N}. \quad (6.13)$$

It's important to emphasize that the quantum criticality condition  $\alpha_G N \approx 1$  indicates that we are dealing with a self-sustained bound state that is on the verge of a quantum phase transition. Furthermore, due to this quantum criticality, the system is characterized by collective Bogolubov modes with small energy gaps, i.e.,  $\Delta\epsilon \sim 1/N$ , which play a role in carrying the entropy of the black hole.

# Chapter 7

## Quantum Nature of Primordial Black Holes

In this section, we present the bulk of this thesis. We discuss the motivation of the work done below and why we believe this may help us in understanding the formation of PBHs when perturbations strained from inflation re-enter the horizon after  $a_{reh}$ . We

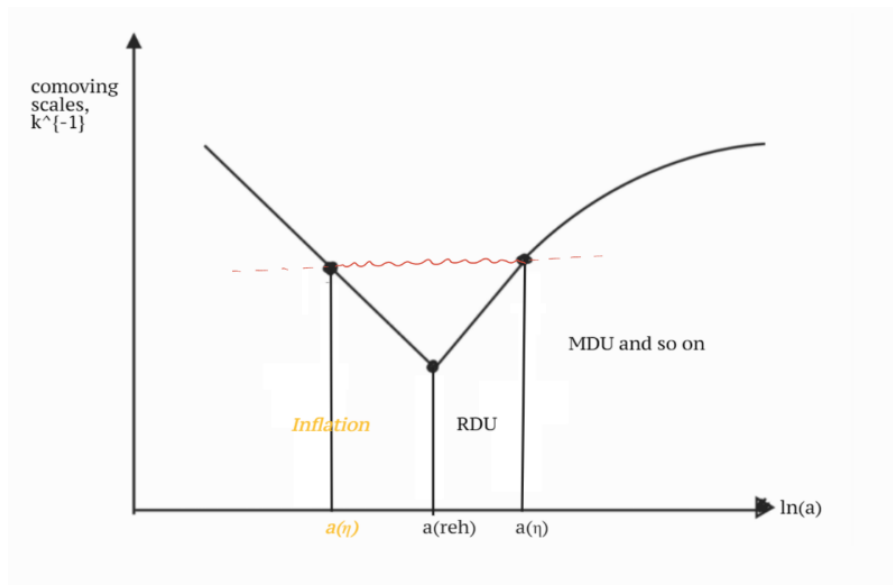


Figure 7.1: A plot depicting the re-entry of perturbation leaving from an inflationary epoch into the radiation-domination universe (RDU). Here, comoving scales run as  $k^{-1}$ . The region before  $a_{reh}$  is the inflationary epoch. The scale factor  $a$  is a function of the conformal time  $\eta$ .

know that the inflationary universe gives rise to extraordinary quantum effects, one of

them is the production of quantum perturbations that ensure the causal mechanism behind decoherence. Also, as the perturbation fields leave the horizon, their vacuum state starts getting occupied due to the particle creation nature of states in a gravitational field.

Therefore, we can conjecture that when the perturbations leave the horizon at a later stage, they don't have enough time to occupy the states before they re-enter. As we have known, these re-entered perturbations are the ones that collapse to form primordial black holes. Hence, if the particle density of the states when they re-enter the horizon is low, they could give rise to the formation of black holes that should be treated as quantum objects due to their low occupation numbers.

To establish this approach, we first need to construct a perturbation field rising from linear scalar perturbations as they evolve into late time structure formation and these density perturbations are the ones that collapse into PBHs. We will deconstruct these perturbation fields into a QFT in curved space to obtain the particle density of the vacuum state as the field re-enters the horizon. We define, primarily, two points of interest on the horizon (with respect to  $a(\eta)$ ) as the exit ("in region") and entry ("out region") of the perturbation field, respectively (Figure 7.1).

## 7.1 Linear Scalar Perturbations

The perturbed Einstein equations give a set of expressions for the inflaton fluctuations  $\delta\phi$  and the gauge-invariant metric perturbations  $\Phi$  and  $\Psi$  (in the longitudinal gauge where  $E = B = 0$ ). At large scales, one can ignore the anisotropic stress and set  $\Phi = \Psi$  so that there are the only two dynamical equations for the inflaton fluctuations and one of the scalar perturbation. Combining them together, we can formulate an equation for a canonical variable as such,

$$u = z\mathcal{R} = a\delta\phi + \frac{\phi'}{\mathcal{H}}\Psi \quad (7.1)$$

where

$$z = \frac{a\phi'}{\mathcal{H}} \quad (7.2)$$

and  $\mathcal{R}$  is curvature perturbation given by

$$\mathcal{R} = \Psi + \frac{H}{\phi'}\delta\phi \quad (7.3)$$

Also,  $\mathcal{H}$  is in its generic definition as  $aH$ . The definition of the curvature perturbation is as (3.27).

So, for this scalar perturbation, we can construct the Mukhanov-Sasaki equation as,

$$u'' + \left(k^2 - \frac{z''}{z}\right)u = 0 \quad (7.4)$$

where

$$\frac{z''}{z} = \mathcal{H}^2(2 + 2\epsilon - 3\eta - 4\eta\epsilon + 2\epsilon^2 - \eta^2 + \xi^2) \quad (7.5)$$

given by the slow-roll parameters.

### 7.1.1 Quantization of the Perturbation Field

Following from the Polarski-Starobinsky paper [6], we introduce the perturbation field computed above and decompose it in terms of a QFT in curved space. We shall follow similar procedures to find the coefficient  $\beta_k$  that will eventually give rise to the particle occupation of the vacuum state in the "out region". Furthermore, we have to mention that we have used the perturbations at linear order.

Quantizing the field above, the Hamiltonian takes the form,

$$H = \int \frac{d^3k}{2} \left[ k(a_k a_k^\dagger + a_k^\dagger a_k) - i \frac{z'}{z} (a_k^\dagger a_{-k}^\dagger - a_k a_{-k}) \right] \quad (7.6)$$

The time-dependent operator (this is being done in Heisenberg representation) is defined to be the usual,

$$a_k = \frac{1}{\sqrt{2}} \left( \sqrt{k} u(\mathbf{k}) + i \frac{1}{\sqrt{k}} p(\mathbf{k}) \right) \quad (7.7)$$

where  $u(\mathbf{k})$  and  $p(\mathbf{k})$  are Fourier transforms of  $u$  and  $p$  respectively. Also,  $p$  is defined to be the conjugate momentum to  $u$  as,

$$p \equiv \frac{\partial \mathcal{L}(u, u')}{\partial u'} = u' - \frac{a'}{a} u \quad (7.8)$$

The term in the Hamiltonian,

$$-i \frac{z'}{z} (a_k^\dagger a_{-k}^\dagger - a_k a_{-k}) \quad (7.9)$$

is responsible for the quantum squeezing of the perturbations. Therefore, this is the term we are interested in.

## 7.2 Bogolubov Coefficients and Particle Density

From (7.7), we can write,

$$u(\mathbf{k}) = \frac{a_k + a_{-k}^\dagger}{\sqrt{2k}}, \quad p(\mathbf{k}) = -i\sqrt{\frac{k}{2}} \left( a_k - a_{-k}^\dagger \right). \quad (7.10)$$

Now, we want to see how the squeezing term affects the time evolution of the system, we have,

$$\begin{pmatrix} a'_k \\ (a_{-k}^\dagger)' \end{pmatrix} = \begin{pmatrix} -ik & \frac{z'}{z} \\ \frac{z'}{z} & ik \end{pmatrix} \begin{pmatrix} a_k \\ a_{-k}^\dagger \end{pmatrix}. \quad (7.11)$$

Solutions to this set of equations is given by,

$$a'_k = -ika_k + \frac{z'}{z} a_{-k}^\dagger, \quad (a_{-k}^\dagger)' = ik a_{-k}^\dagger + \frac{z'}{z} a_k \quad (7.12)$$

This is a Bogolubov transformation with the Bogolubov coefficients,  $-ik$  and  $\frac{z'}{z}$ . We have to note that  $z$  is real, therefore its complex conjugate is itself. We can relate these coefficients to the ones presented in the  $\alpha - \beta$  formalism,

$$-ik = \alpha_k e^{-ik\eta}, \quad \frac{z'}{z} = \beta_k e^{ik\eta} \quad (7.13)$$

From here, we can find the coefficient needed to find the particle density  $|\beta_k|^2$ .

$$|\beta_k|^2 = \beta_k^* \beta_k = \left( \frac{z'}{z} \right)^2 \quad (7.14)$$

Furthermore, we know the particle density can be calculated by running the integration over this quantity with an inverse volume normalization factor to get rid of divergences. Therefore, we use [4],

$$N = \frac{1}{(2\pi a)^3} \int d^3k |\beta_k|^2 = \frac{1}{(2\pi a)^3} \int d^3k \left( \frac{z'}{z} \right)^2 \quad (7.15)$$

We have the expression for  $z$  as:

$$z = \frac{a\phi'}{\mathcal{H}}. \quad (7.16)$$

To find  $z'$ , we differentiate this expression with respect to  $\eta$ :

$$z' = \frac{d}{d\eta} \left( \frac{a\phi'}{\mathcal{H}} \right). \quad (7.17)$$

We have a form for the  $\frac{z'}{z}$  term,

$$\frac{z'}{z} = \frac{a'\phi' + a\phi'' - \frac{\mathcal{H}'}{\mathcal{H}}a\phi'}{a\phi'}. \quad (7.18)$$

From here, we can decipher each of the terms separately to find the expression for  $\frac{z'}{z}$ . This will help us understand the dependence of the cosmological parameters on  $\frac{z'}{z}$ :

$$\frac{z'}{z} = \mathcal{H} - \frac{\mathcal{H}'}{\mathcal{H}} + \frac{\phi''}{\phi'} \quad (7.19)$$

Due to the slow-roll conditions,  $\phi''$  is typically small compared to other terms in the inflationary dynamics. The smallness of  $\phi''$  in slow-roll inflation indicates that the inflaton field experiences a gentle acceleration. This slow acceleration contributes to the prolonged period of inflation, allowing for the expansion of the universe and the generation of the required density fluctuations.

Overall, in slow-roll inflation,  $\phi''$  is expected to be small compared to other terms, reflecting the slow and gradual evolution of the inflaton field during the inflationary epoch. Therefore, we can neglect this term from the expression of  $\frac{z'}{z}$ .

$$\frac{z'}{z} = \mathcal{H} - \frac{\mathcal{H}'}{\mathcal{H}} \quad (7.20)$$

Simplifying further, we get:

$$\left(\mathcal{H} - \frac{\mathcal{H}'}{\mathcal{H}}\right)^2 = \mathcal{H}^2 - 2\mathcal{H}' + \frac{\mathcal{H}'^2}{\mathcal{H}^2} \quad (7.21)$$

However, we should note that the effects of the slow-roll condition may differ at the end of inflation for which we are considering  $a = 1$  and  $\eta = 0$ .

### 7.2.1 Exiting the Horizon

Let's compartmentalize the model for better understanding: On the cyan horizon line in Figure 7.2, we have

$$\left(\frac{z'}{z}\right)^2 = \left(\mathcal{H} - \frac{\mathcal{H}'}{\mathcal{H}}\right)^2 = \mathcal{H}^2 - 2\mathcal{H}' + \frac{\mathcal{H}'^2}{\mathcal{H}^2} \quad (7.22)$$

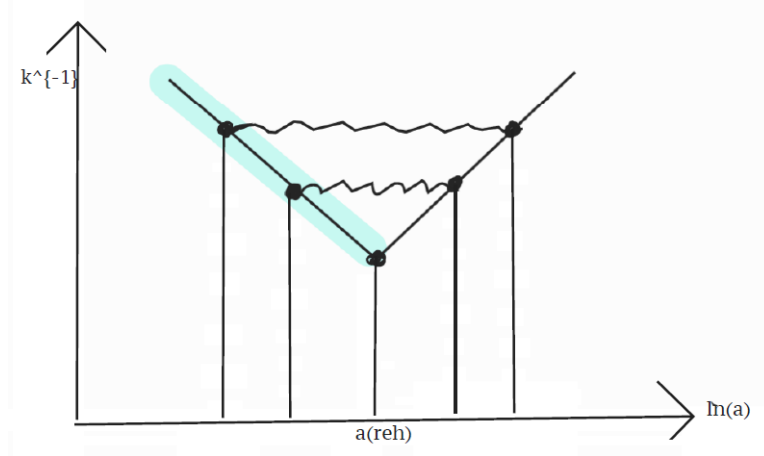


Figure 7.2: Perturbation fields exiting the horizon at an earlier and later stage of inflation, respectively.

We make further assumed relationships such as,

$$a_{inf} \sim \frac{1}{1-\eta}, \quad \mathcal{H} = \frac{1}{1-\eta}, \quad \mathcal{H}' = \frac{1}{(1-\eta)^2} \quad (7.23)$$

This parametrization allows us to keep the reheating point (end of inflation) at  $a = 1$  and therefore, helps avoid the singularity at  $\eta = 0$ .

Hence, we find the particle density on the horizon line,

$$dN_{out} = \frac{1}{(2\pi a_{inf})^3} |\beta_k|^2 d^3k = 0 \quad (7.24)$$

which is good as it matches our assumption. The vacuum states only occupy when the modes leave the horizon, therefore, we find the states to be empty on the horizon line.

### 7.3 Mukhanov-Sasaki Equation: Solution for Inflationary Models

Now, we cannot define the modes outside the horizon with the same mathematical equation as it leads to uncertainties due to the different mechanisms. As introduced in Chapter 5, the field modes were defined in the paper by Starobinsky-Polarski to have the form:

$$f_k = \frac{u_k + v_k^*}{\sqrt{2k}} \quad (7.25)$$

Now, as per our model,  $u_k$  and  $v_k^*$  are related to the Bogolubov coefficients, respectively as

$$u_k = \alpha_k e^{-ik\eta}, \quad v_k^* = \beta_k e^{ik\eta} \quad (7.26)$$

Considering the origin of these fields, at sub-Hubble scales  $k\eta \gg 1$ , therefore we can assume the  $\alpha_k$  term is negligible and express the field modes as,

$$f_k = \frac{\beta_k e^{ik\eta}}{\sqrt{2k}}$$

For modes with wavelengths outside the Hubble radius, the general solution of the Mukhanov-Sasaki equation has the following form in terms of the field modes.

$$f_k = C_1 z + C_2 z \int \frac{d\eta}{a^2(\eta)} \quad (7.27)$$

Now,

$$|f_k|^2 = f_k^* f_k = \frac{\beta_k e^{ik\eta}}{\sqrt{2k}} \frac{\beta_k^* e^{-ik\eta}}{\sqrt{2k}} = \frac{|\beta_k|^2}{2k} \quad (7.28)$$

Therefore,  $|\beta_k|^2 = 2k|f_k|^2$ .

For inflationary models,

$$C_1 = \frac{H_k}{\sqrt{2k^3}}, \quad C_2 = \frac{-ik^{\frac{3}{2}}}{\sqrt{2}H_k} \quad (7.29)$$

where  $H_k$  is the slowly varying Hubble radius.

Therefore,

$$|\beta_k|^2 = 2k \left\{ \left( \frac{H_k}{\sqrt{2k}} z \right)^2 - \left( \frac{ik^{\frac{3}{2}} z}{\sqrt{2}H_k} \int \frac{d\eta}{a^2(\eta)} \right)^2 \right\} \quad (7.30)$$

In the parametrization (7.23) we used before, we find

$$|\beta_k|^2 = \frac{1}{k^2} + \frac{k^4(1-\eta)^6}{9} \quad (7.31)$$

### 7.3.1 Quasi-isotropic Mode and Decaying Mode

The first term in (7.31) is the quasi-isotropic mode, also called the growing mode. It comes as a consequence of the first term in (7.27). The second term is called the decaying mode. During horizon exit, both of these modes are of equal order, however, when the perturbation field spends time outside the horizon, it leads to decoherence and the decaying mode quickly becomes negligible. Therefore, at larger scales, for perturbation



modes that leave the horizon earlier, the growing modes are of precedence. This is because in that stage,  $k_{CMB} \ll k_{PBH}$ , therefore we can see that the inverse square term would contribute more. Hence, we can consider a classicalization limit, and find the particle density accordingly.

We define the following parametrization for the radiation domination era,

$$a_{rad} \sim \eta + 1, \quad \mathcal{H} = \frac{1}{\eta + 1} \quad (7.32)$$

Hence, using this we find,

$$dN_c = \frac{1}{(2\pi a)^3} \left( \frac{1}{k^2} \right) d^3k = \frac{k^3}{C_1} dk \quad (7.33)$$

where  $C_1$  is a constant.

If we consider decoherence time, i.e. classicalization of the perturbation field, the particle density would decrease as more classicalization takes place. This is due to quantum effects of the perturbation fields that gives rise to particle production in the vacuum start to cease. For example, in the following plot we can see that  $dN_1$  will be greater than  $dN_2$  in the classical limit.

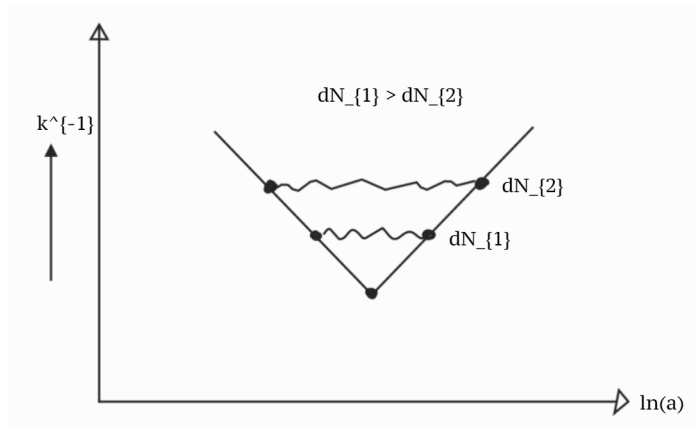


Figure 7.3: The particle density in the classicalization limit seems to decrease with decreasing  $k$  as  $dN_2 < dN_1$ .

However, in popular literature, the quasi-isotropic mode is only considered as these perturbation fields are constructed from a decohering point of view. But as we move to a more earlier patch where  $k$  is greater and decoherence time is short, we believe the extra second term in the expression in (7.31) should be considered, so that

$$|\beta_k|^2 \sim \frac{k^4(1-\eta)^6}{9} \quad (7.34)$$

Therefore, for fields that leave the horizon very late in the inflationary era, we consider the growing mode to take precedence due to its  $k^4$  dependence. Furthermore, we can ignore the effect of  $\eta$  here as it is incomparable to the high  $k$  effective in this scenario.

We find,

$$dN_q = \frac{1}{8\pi^3 a^3} \left\{ \frac{k^4(1-\eta)^6}{9} \right\} d^3k \quad (7.35)$$

Recalling the parametrization in (7.23), we can implement the relationships as,

$$dN_q = \frac{1}{8\pi^3} \frac{(1-\eta)^9 k^4}{9} k^2 dk = \frac{C_2}{k^3} dk \quad (7.36)$$

where  $C_2$  is a constant.

For both of the measures, we used the relationship of  $k$  with the conformal time at horizon crossing to obtain an estimate of the particle density evolution at collapse of the perturbation field during horizon entry.

$$\mathcal{H} \sim k \sim \frac{1}{1-\eta} \quad (7.37)$$

Furthermore, we need to consider the fact that as decoherence time is short, the modes do not classicalize upon horizon entry and therefore, we consider the evolution of the scale factor for this patch to be similar to the one of inflationary models.

Now, for this patch of the model, we see that as we go further towards higher  $k$ , we have smaller  $dN$  until at the critical point (point where inflation ends), we have null production as, theoretically, the modes do not spend any time outside the horizon. This is testament to our claim that in very early universe conditions, we have the production of very small primordial black holes that should be treated as quantum objects. This is in contrast of what is usually done, i.e. treating these black holes as semi-classical. Therefore, we can start explaining these black holes in a fully quantum-mechanical framework.

## 7.4 Null Particle Production at Reheating

In this section, we verify our model in a two-fold way in order to make it more concrete. We first calculate the particle production in the vacuum at reheating. Reheating is when inflation ends ( $\eta = 0$ ).

$$\mathcal{H} \sim k \sim \frac{1}{1-\eta} \sim 1 \quad (7.38)$$

We find,

$$N_q = C_3 \left( \frac{1}{k^2} - 1 \right) \quad (7.39)$$

This is in relation to the fact that  $k$  is maximized at  $\eta = 0$  and decreases as we move into the radiation-domination era as can be seen from Figure 4.1.

We see in (7.39) that at  $\eta = 0$ , we do not have any particle production. This is in coherence with (7.24) as well as intuitively, given that the perturbation fields do not spend time outside of the horizon.

Furthermore, we can plot the relationship of the terms in (7.31) and track the switch between the preceding terms. We represent the relationship of the particle number  $N$  at differing  $k$ .

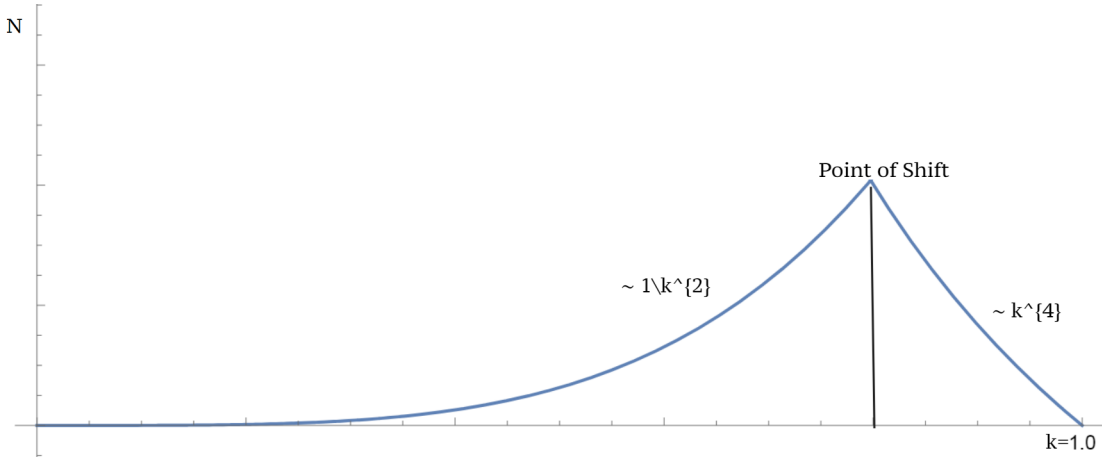


Figure 7.4: In this plot we see that the two terms do have a point of shift in regards to how they contribute to the particle number. The scale on this plot has been taken arbitrarily due to the lack of phenomenological data. Also  $k$ , in essence, cannot be discrete. This plot shows that with decreasing  $k$ , we have the quantum regime ( $k^4$ ) that contribute to  $N$  and eventually as  $k$  reaches the classicalization limit, the quasi-isotropic mode takes over and the fields lose quantum coherence, hence, particle production in the vacuum ceases. At  $k = 1$ , we have zero particle production.

## 7.5 The Corpuscular Perspective

We can also take into account the corpuscular picture to strengthen our claim regarding these quantum primordial black holes. From (6.12), we can relate the particle density

number with the occupation number of the gravitons.

$$N \sim \frac{M^2}{M_P^2} \tag{7.40}$$

We can consider,

$$M^2 = (k^2 N_q)^2 = \left\{ C_3 \left( 1 - \frac{1}{k^2} \right) \right\}^2 \tag{7.41}$$

Here,  $k$  is very high at the time of primordial black hole formation, therefore, we clearly see from the relation posed in Chapter 6.1 that these black holes that form in this setting cannot be considered as classical objects. They do not produce an occupation number which is  $N \gg 1$  and therefore should be treated from a quantum setup.

# Chapter 8

## Conclusion

The work done in this thesis is attested to show that our treatment of primordial black holes should change, theoretically, at least when they formed near the end of inflation. We see that in the very early universe, these black holes that form from scalar perturbations left from inflation are quantum in nature. Considering the energy scales, along with the size of the universe in that era, we can assume that the mass of these primordial black holes will be very small to consider them as exhibiting classical physics.

Furthermore, the particle density of the occupied vacuum states of these perturbation fields amount to very low occupation. Hence, we can conclude that the density perturbations that re-enter the horizon earliest will form quantum primordial black holes.

This model has been carried using several initial conditions. We start off with using linear density perturbations in the longitudinal gauge. This work could be analysed more critically by adjusting non-linear terms in our construction of the perturbation fields. We should also note the slow-roll condition we considered with  $\phi''$  being negligible in comparison to the other terms in the construction of  $\frac{z'}{z}$ ; the possible effects of the end of inflation to this term are going to be the topic of further investigations.

Moreover, including phenomenological data may help us quantify  $N$  at the point of shift. This could serve interesting to see the maximum mass range of formed primordial black holes and correspond the theoretical calculation with the observed assumption.

Interestingly, the bound on  $k$  due to the end of inflation shall provide a lower bound to the mass of the primordial black holes formed. We could imply these restrictions to analyze alongside phenomenological data to source an outcome of the validity of these results. This could also be implied for maximum  $N$ .

Another exciting result from the plot in Figure 7.4 is that we can see that the quantum

regime is short-lived in comparison to the classical regime. Therefore, it would make sense why we have decoherence of the quantum fluctuations as they leave the horizon during inflation. However, primordial black holes can still potentially be formed during the quantum regime as quantum fluctuations re-enter the horizon at this stage.

Furthermore, this generalized model could potentially be extended to other inflationary scenarios to see if indeed this framework is well-suited to describe primordial black holes. This setup utilizes scale-invariant metric perturbations, therefore, it could be used to describe other early universe models that consist of a similar structure.

# Bibliography

- [1] S. Hawking, *Mon. Not. Roy. Astron. Soc.* **152** (1971), 75 doi:10.1093/mnras/152.1.75
- [2] B. J. Carr and S. W. Hawking, *Mon. Not. Roy. Astron. Soc.* **168** (1974), 399-415 doi:10.1093/mnras/168.2.399
- [3] A. Giusti, doi:10.6092/unibo/amsdottorato/8751
- [4] L. H. Ford, [arXiv:gr-qc/9707062 [gr-qc]].
- [5] O. Özsoy and G. Tasinato, *Universe* **9** (2023) no.5, 203 doi:10.3390/universe9050203 [arXiv:2301.03600 [astro-ph.CO]].
- [6] D. Polarski and A. A. Starobinsky, *Class. Quant. Grav.* **13** (1996), 377-392 doi:10.1088/0264-9381/13/3/006 [arXiv:gr-qc/9504030 [gr-qc]].
- [7] N. D. Birrell and P. C. W. Davies, Cambridge Univ. Press, 1984, ISBN 978-0-521-27858-4, 978-0-521-27858-4 doi:10.1017/CBO9780511622632
- [8] G. Dvali and C. Gomez, *Fortsch. Phys.* **61** (2013), 742-767 doi:10.1002/prop.201300001 [arXiv:1112.3359 [hep-th]].
- [9] R. Casadio, A. Giugno and A. Giusti, *Phys. Lett. B* **763** (2016), 337-340 doi:10.1016/j.physletb.2016.10.058 [arXiv:1606.04744 [hep-th]].
- [10] R. Casadio, A. Giugno, O. Micu and A. Orlandi, *Phys. Rev. D* **90** (2014) no.8, 084040 doi:10.1103/PhysRevD.90.084040 [arXiv:1405.4192 [hep-th]].
- [11] G. Calcagni, M. G. Di Luca and T. Fodran, *PoS CORFU2021* (2022), 317 doi:10.22323/1.406.0317 [arXiv:2202.13875 [gr-qc]].
- [12] V. Mukhanov, Cambridge University Press, 2005, ISBN 978-0-521-56398-7 doi:10.1017/CBO9780511790553
- [13] R. Casadio, A. Giugno, O. Micu and A. Orlandi, *Entropy* **17** (2015), 6893-6924 doi:10.3390/e17106893 [arXiv:1511.01279 [gr-qc]].

- [14] A. H. Guth and S. Y. Pi, Phys. Rev. Lett. **49** (1982), 1110-1113 doi:10.1103/PhysRevLett.49.1110
- [15] S. W. Hawking, Commun. Math. Phys. **43** (1975), 199-220 [erratum: Commun. Math. Phys. **46** (1976), 206] doi:10.1007/BF02345020
- [16] G. Dvali and C. Gomez, Eur. Phys. J. C **74** (2014), 2752 doi:10.1140/epjc/s10052-014-2752-3 [arXiv:1207.4059 [hep-th]].
- [17] A. H. Guth and S. Y. Pi, Phys. Rev. Lett. **49** (1982), 1110-1113 doi:10.1103/PhysRevLett.49.1110
- [18] A. A. Starobinsky, JETP Lett. **30** (1979), 682-685
- [19] B. J. Carr and J. E. Lidsey, Phys. Rev. D **48** (1993), 543-553 doi:10.1103/PhysRevD.48.543
- [20] T. Papanikolaou, [arXiv:2202.12140 [astro-ph.CO]].
- [21] A. H. Guth, Phys. Rev. D **23** (1981), 347-356 doi:10.1103/PhysRevD.23.347
- [22] B. J. Carr, Astrophys. J. **201** (1975), 1-19 doi:10.1086/153853